UNITED STATES DEPARTMENT OF THE INTERIOR

U.S. GEOLOGICAL SURVEY

GEOCHEMICAL AND BIOGEOCHEMICAL SURVEYS NEAR THE MINERAL AND VALLEY VIEW HOT SPRINGS KNOWN GEOTHERMAL RESOURCE AREAS NORTHERN SAN LUIS VALLEY, COLORADO

By

Margaret E. Hinkle* and James A. Erdman*

Open-File Report 95-569

1995

* U.S. Geological Sruvey, P.O. Box 25046, Mail Stop 973, Denver, CO, 80225

CONTENTS

ABSTRACT

The Mineral Hot Springs and Valley View Hot Springs Known Geothermal Resurce Areas are located in the northern part of the San Luis Valley, Colorado. To seek evidence for possible extensions of these hot spring systems, the U.S. Geological Survey conducted surveys of the northern San Luis Valley utilizing surficial geochemical and biogeochemical exploration techniques. The objective of the study was to see if analyses of surficial soil samples, soil gases, and rabbitbrush (genus Chrysathamnus) could detect extensions of the hot springs.

Many of the geochemical and biogeochemical anomalies were observed to be associated with the large fault systems of the valley. Soil and soil-gas data suggested six causes for the various geochemical anomalies: (1) epithermal sulfide mineralization in carbonate bedrock, (2) fossil and possible present-day geothermal activity with accompanying hot-spring deposition, (3) acid alteration along faults containing sulfide mineralization, (4) Mo and Cu sulfide mineralization, probably related to the Rito Alto stock, (5) Ag and Hg in hot-spring sinter deposits, and (6) migration of He through permeable faults. The surveys did not detect any extensions of the Valley View Hot Springs KGRA. However, some of the anomalies on the west side of the valley could be indirectly related to Mineral Hot Springs KGRA.

Most of the element-concentration anomalies in soil samples collected south of the town of Villa Grove are probably due to metals carried by Kerber Creek from old mines of the Bonanza mining district.

Anomalous concentrations of Li, B, and Mn in rabbitbrush combined with high soil-Hg concentrations and anomalous CO_2 concentrations in soil gases collected nearby suggest a geothermal heat source beneath the low hills of Precambrian granites just west of Mineral Hot Springs. The areal coincidence of surficial anomalies with concealed subsurface faults detected by a resistivity survey indicated the utility of surficial geochemical-biogeochemical surveys--a significant result of the investigation.

INTRODUCTION

The San Luis Valley lies between low foothills of the San Juan Volcanic Field to the west and the steeply-rising Sangre de Cristo Range to the east (fig.1). Two Known Geothermal Resource Areas (KGRAs) exist in the northern San Luis Valley. The first KGRA, Mineral Hot Springs (spring-water temperatures 32-55^{0}C) (Barrett and Pearl, 1978), is located in valley fill about midway between the San Juan Volcanic Field on the west side of the valley and the Sangre de Cristo Range on the east, about 9 km south of the town of Villa Grove. The second KGRA, Valley View Hot Springs (spring-water temperatures 31-33^{0}C), lies on the prominent Sangre de Cristo fault, along the west side of the Sangre de Cristo Range.

At the surface, both the Valley View and Mineral Hot Springs KGRAs appear to be limited to the immediate areas of their hot springs. As a part of their geothermal energy program, the U.S. Department of Energy asked the USGS to conduct the geochemical and biogeochemical surveys described in this report, to determine if any extensions to the KGRAs could be detected by surficial sampling. The area investigated in this report encompassed the northern part of the valley, between 38^{0}07'30" - 38^{0}15' N latitude and about 105^{0}47'30" - 106^0 W longitude.

Regional geology

The San Luis Valley is an east-dipping half graben and is the geomorphic expression of the Rio Grande Rift in southern Colorado. The northern part of the San Luis Valley is cut by several faults (Tweto et al., 1976; Scott et al., 1978). Major faults trend primarily northwestward and have been well-mapped in the surrounding mountains, however, several subsurface faults are concealed by alluvium in the center of the valley.

The prominent late-Tertiary age Sangre de Cristo fault, a part of the Rio Grande Rift system, is the bounding fault of the Sangre de Cristo Range; the fault runs the length of the west side of the range and cuts obliquely across structural features in the valley and the range. The Holocene Villa Grove fault zone trends northwesterly across the northern San Luis Valley from the vicinity of Valley View Hot Springs (Knepper, 1974, 1976; Knepper and Marrs, 1971). Rocks and sediments underlying the western side of the valley are cut by the Kerber, Noland, Clayton, and Villa Grove faults which extend northwesterly from the vicinity of Mineral Hot Springs (Bridwell, 1968; Scott et al., 1978) (fig. 1). The Laramide Kerber Creek-Major Creek fault zone crosses the valley from Major Creek in the Sangre de Cristo Mountains on the east to the Kerber and Noland faults on the west (Burbank and Henderson, 1932; Burbank and Goddard, 1937).

Geochemical anomalies related to mineral-resources

Part of the Sangre de Cristo Wilderness Area lies along the eastern border of the area studied in this investigation. Exposed rocks in the Wilderness Area consist of Precambrian crystalline rocks and upper Paleozoic clastic sedimentary rocks, with several fault-bounded slivers of lower Paleozoic sedimentary rocks near the western boundary, especially in the area of Valley View Hot Springs (Johnson et al., 1984b). A geochemical survey indicated several areas where stream sediments draining the western side of the Sangre de Cristo Mountains contain anomalous concentrations of metallic elements (Zimbelman, 1989). Anomalies of Ag, Pb, Cu, Zn, and Mo were found scattered along the mountain front along the east side of the study area, in drainages downstream from old mines and prospects.

Biogeochemistry

The San Luis Valley is unusually arid for its altitude. Annual precipitation at the town of Saguache (approximately 2350 m elevation) averages about 22 cm, the valley is the highest region in the United States to receive so little moisture (Doesken and McKee, 1989). The northern part of the valley supports a shrub-grassland characterized by two species of rabbitbrush (genus *Chrysothamnus*) on uplands where soils are non-saline and relatively non-alkaline. The valley floor supports greasewood (genus *Sarcobatus*) where conditions are more alkaline and the water table occurs near the surface (Dixon, 1989). Greasewood tolerates soils containing as much as nine percent salt. For the most part the soils in the study area are well-drained and non-calcareous.

Known Geothermal Resource Areas

The Mineral Hot Springs and Valley View Hot Springs KGRAs are among several geothermal areas found along the Rio Grande Rift. These KGRAs are located within

sedimentary basins and are heated by the normal geothermal gradient. The hot waters migrate to the surface along the conduits provided by the tectonic activity along the rift (Swanberg, 1979).

Subsurface water temperatures calculated from spring water analyses are 70^0-90^0C for Mineral Hot Springs and 40^0-50^0C for Valley View Hot Springs (Barrett and Pearl, 1976, 1978). Both springs deposit calcareous sinter (Mineral Hot Springs--40% Ca, Valley View Hot Springs--38% Ca), further evidence that subsurface water temperatures are low (White, 1970). Although the temperatures of the geothermal waters are too low to use for geothermal electricity production, waters of these temperatures can be used for space heating, agriculture, and industry.

The two springs differ in both temperature and chemistry. The waters of Mineral Hot Springs have higher concentrations of total dissolved solids and of geothermally-significant elements such as As, B, and Cl than the waters of the Valley View Hot Springs (table 1; Barrett and Pearl, 1976). Sinter deposited by Mineral Hot Springs has higher concentrations of Mn, As, Be, Li, Sr, and Hg than sinter from Valley View Hot Springs, whereas the sinter of Valley View Hot Springs is higher in Al, K, Ti, Ag, Ce, Co, Cr, Cu, Ni, V, Y, and Zn than sinter from Mineral Hot Springs (table 2; Motooka et al., 1994).

Zohdy and Bisdorf (1993) conducted a direct-current resistivity survey, consisting of 30 deep Schlumberger soundings, in the area of Mineral Hot Springs. The resistivity survey covered an area of approximately 10 by 15 kilometers (fig. 2). East-west trending faults were found beneath the alluvium south of Villa Grove. The Mineral Hot Springs were found to occur above a graben-like structure over a deeply seated, relatively low resistivity zone bounded by two deep faults.

GEOCHEMICAL AND BIOGEOCHEMICAL SURVEYS

Soil and soil-gas survey

A total of 396 samples of - 80 mesh surficial soils and 395 soil-gases from 0.7m depths were collected along road traverses at 0.1mi (160m) intervals; many of these samples were collected in traverses over faults where plants were also collected. The soil gases were analyzed for CO_2, O_2, and N_2 by gas chromatography and for He by mass spectrometry (Hinkle, 1993). The soil samples were analyzed for Hg by atomic-absorption spectrophotometry. Hydrogen-ion contents were calculated from pH measurement of soil slurries [pH = -log H+ (moles/liter)]. The primarily secondary oxide-related concentrations of Ag, As, Cd, Cu, Mo, Pb, Sb, and Zn in soils were measured by a partial-extraction induction-coupled plasma (ICP) method; the partial-extraction method does not measure metal content related to the silicate lattice of common rock-forming minerals. Descriptions of the procedures and analytical results from the samples were summarized by Motooka et al. (1994).

Data from the combined soil and soil-gas analyses were used for statistical analysis (table 3). Values listed as "L" (below the lowest level of determination) in table 3 were converted to real numbers by arbitrarily multiplying the lowest detectable value by 0.1. Concentrations of Ag and Sb were retained in the data set, although less than 50% of the samples had detectable values. Correlation coefficients for the unqualified and replaced values indicated strong relationships ($r \geq .50$) between some of the elements--for example, As with Sb and Pb; Pb with Cd;

and Pb with Sb and Zn (table 4). Analytical data were from all the sample media were converted into the U.S. Geological Survey GSPOST format for plotting (Selner and Taylor, 1992).

Plots of the combined soil and soil-gas data showed anomalous concentrations (>95th percentiles of concentrations) of metals related to sulfide minerals, Hg, and hydrogen-ion in soils, and CO_2 and He in soil gases clustered in several locations of the northern San Luis Valley (Hinkle, 1993; Motooka et al., 1994). Many of these anomalous areas were located over the large fault systems of the valley. Other anomalies appeared to be related to past mining activity.

On the east side of the valley, anomalous concentrations of He, Ag, Cd, and H^+ were located along the Villa Grove fault zone northwest of Valley View Hot Springs. Along the Sangre de Cristo fault, anomalous concentrations of He, Ag, Cu, Cd, Mo, Pb, Sb, and H^+ were found downslope from Orient Canyon (the Orient Mine is at the mouth of Orient Canyon); anomalies of CO_2, Cu, and Mo were located in the vicinity of Garner Creek south of Valley View Hot Springs. Anomalous He, Ag, and Mo concentrations at Valley View Hot Springs itself appeared to be related primarily to the Sangre de Cristo fault.

On the west side of the valley, anomalous concentrations of most of the elements measured in the study, especially As and Sb, were clustered around the hills in the area of the "eastern anticline" (Burbank and Henderson, 1932; Bridwell, 1968; Knepper, 1974). Anomalies of He, CO_2, Zn, Hg, and H^+ were found over the Kerber and Noland faults.

Scattered anomalous concentrations of He, CO_2, Cu, Cd, Mo, Pb, and Hg were located within the concealed Kerber-Major Creek fault zone that crosses the central part of the valley (Burbank and Goddard, 1937; Knepper, 1974; Davis and Stoughton, 1979). Although concentrations of He and Hg were higher than average at some of the sites around Mineral Hot Springs, the hot springs area did not appear significantly geochemically different from the rest of the study area.

Concentrations of He, Ag, Cu, Cd, Mo, Pb, Zn, Hg, and H^+ were anomalous in samples collected south of the town of Villa Grove. Many of the anomalous sample sites were located within the Kerber Creek flood plain, indicating that the anomalous metals probably are related to contamination from old mines of the Bonanza mining district about 25 km west of Villa Grove. The mines produced Cu, Pb, Zn, and Ag from about 1880-1920 (Burbank and Henderson, 1932).

Biogeochemical survey

One-hundred-thirty-nine samples of rabbitbrush (genus *Chrysothamnus*), which dominates the valley, were collected in an approximate grid. More closely-spaced sample sites were positioned along traverses across the mapped faults or fault zones that might serve as conduits for mineralizing and geothermal fluids. Two forms of rabbitbrush were recognized, a more common form that had a grayish appearance and a less common form that was more green. The gray form was identified as (*C. parryi* ssp. *howardii*) and the green form was identified as (*Chyrsothamnus nauseousus* ssp. *consimilis*. Field notes included information on the color form, and subsequent analytical results show no species differences. The plant samples were analyzed by neutron activation analysis (INAA) for 35 elements, inductively coupled plasma-

atomic emission spectroscopy (ICP-AES) for 30 elements, and prompt-gamma INAA for B. Results of the rabbitbrush sampling were summarized in Erdman and Van Trump (1993).

Sites with anomalous concentrations in rabbitbrush of Li and Mn (>6.1 ppm and 1200 ppm, repectively, in ash) and B (>62 ppm in dried plant material) were located near sites with anomalous concentrations of Hg in soils (30 ppb) and CO_2 in soil gases (0.53 % by volume), particularly in the low hills just west of Mineral Hot Springs. This combination of anomalous concentrations suggests the occurrence of a geothermal heat source in the Precambrian granites of the area. Several other distinct geochemical spatial patterns, probably unrelated to geothermal activity, were also revealed (Erdman et al., 1993).

DISCUSSION--SOIL AND SOIL-GAS ANOMALIES

Possible explanations for the clusters of anomalous elments are epithermal sulfide mineralization in carbonate bedrock, fossil and present-day geothermal activity with accompanying hot-spring deposition, acid alteration along faults containing sulfide mineralization, Mo and Cu sulfide mineralizatiсn, Ag and Hg deposition in hot-spring sinters, and upward migration of He through permeable faults. Many anomalous sample sites (> 95th percentiles of concentrations) were located over faults (figs. 3-7). Some of the element anomalies seen in this investigation are similar to anomalies seen at the Roosevelt Hot Springs, Utah, KGRA (Christensen et al., 1983; Hinkle and Copp, in press). Because total element concentrations (oxide- and silicate -related) were not measured for the majority of the samples, the detrital component of the soil-sample data, which might be indicated by total element analyses, could not be determined.

Epithermal sulfide mineralization: Anomalous concentrations of As, Sb, Pb, and Cd (table 3) primarily represent epithermal-sulfide mineralization within carbonate bedrock (figs. 3-4). The largest cluster of anomalous sites is located around the eastern and southern sides of the hills in the southern part of the "eastern anticline" (Burbank and Henderson, 1932; Bridwell, 1968; Knepper, 1974) where carbonate bedrock occurs. Samples in this area had the highest concentrations of As and Sb measured in this survey. Although high concentrations of As in soils might reflect high-temperature fluid flow-controlling fractures in the area of the eastern anticline, a situation similar to that at Roosevelt Hot Springs KGRA (Christensen et al., 1983; Hinkle and Copp, in press), epithermal mineralization in carbonate bedrock of the eastern anticline is more likely than deposition from brines.

Fossil and present-day geothermal activity: Anomalous concentrations of N_2, O_2, CO_2, and Zn (figs. 4-5) represent fossil and present-day geothermal activity with accompanying hot-spring deposition. Samples with high concentrations were located near the Noland fault on the west side of the valley and scattered over the Sangre de Cristo fault. A few anomalous sites in the center of the valley were located over faults identified by Zohdy and Bisdorf (1993) within the Kerber Creek-Major Creek fault zone. The CO_2 and Zn indicate upward movement of fluid through faults overlying a geothermal source and release of CO_2 at the surface. Zinc is one of the elements deposited with siliceous material at locations of liquid discharge, fluid mixing or boiling at the Roosevelt Hot Springs KGRA (Christensen et al., 1983; Hinkle and Copp, in press).

Anomalous concentrations of CO_2 and He in soil gases and Hg in soils are often associated with geothermal activity. A plot of concentrations above the 95th percentile for these elements (table 3) shows anomalous CO_2 and Hg at and near Valley View Hot Springs (fig. 6). Nearby soil-gas samples have anomalous He that probably is related to the Sangre de Cristo fault. Whether or not He, CO_2, and Hg are anomalous directly over the Mineral Hot Springs area is not known because we were unable to collect samples there. Some of the samples collected near Mineral Hot Springs had anomalous He, Hg, or CO_2, but a larger number of samples were not anomalous.

Valley View Hot Springs lies on the Sangre de Cristo fault, which provides a channelway and outlet for elements to rise from the geothermal source. In contrast, the Mineral Hot Springs geothermal source may have an impermeable cap of clay or siliceous material that restricts the upward movement of volatiles from the geothermal source to faults and fractures. Resistivity measurements at 500-600 m depth in the area of Mineral Hot Springs indicated the possibility of a layer of fine sediments in a matrix cemented by the action of geothermal fluids (Zohdy and Bisdorf, 1993). Although the concentration of Hg in sinter deposited by Mineral Hot Springs is slightly higher than that of Valley View Hot Springs (table 2), an impermeable cap restricting the upward movement of gases and fluids at Mineral Hot Springs would explain the lower concentration of Hg in soils there than at Valley View Hot Springs. An impermeable cap would also explain the scattered distribution of anomalous He concentrations around Mineral Hot Springs. Similar distributions of below-average concentrations of He and above-average concentrations of Hg occurred over an opal-cemented fault at Roosevelt Hot Springs (Hinkle and Copp, in press).

A large number of sites with anomalous He, CO_2, and Hg are located near and along the Noland fault and between the Noland and Kerber faults. Similar geothermal anomalies are also located in the eastern anticline area. These anomalies indicate that geothermal activity occurred in both these areas in the past and that present geothermal activity is possible, especially in the Noland fault area where N_2 concentrations are also anomalous.

Some of the faults probably are saturated with water. Observations on the vegetation by D.A. Lindsey (oral communication, 1992), who mapped the geology in the eastern part of the study area, as well as those by Erdman, indicate that groundwater seepage and drainage disruption occurs intermittently at the base of the scarps along the Villa Grove fault zone. These and other faults may be filled with clays and silica minerals. Very low concentrations of N_2 and O_2 in soil gases were seen at several sites over the Villa Grove fault zone and also at some sites in the center of the valley (Hinkle, 1993, fig. 4); these sites were probably also saturated with water.

High N_2/O_2 concentration ratios in soil gases can be evidence for O_2 depletion. The N_2/O_2 ratio was exceptionally high at several sites along the Villa Grove fault zone (fig. 8). The N_2/O_2 ratio for air is 3.74; the ratio for soil gases at these anomalous sites was greater than the mean for the area plus twice the standard deviation (>3.76 + 0.62). Very low concentrations (<25th percentile) of O_2 in soil gases coincided with very high (>95th percentile) concentrations of hydrogen-ion content in soils at several of the anomalous sites (Hinkle, 1993; Mctooka et al., 1994). The inverse relationship of O_2 with H^+ concentrations probably indicates O_2

loss and subsequent formation of sulfuric acid during weathering of sulfide minerals in water-filled faults.

Very high concentrations, over about 80% N_2 or 22% O_2 in soil gases (>99th percentiles), were observed primarily over the Noland fault and in the area where the Noland, Clayton, and Villa Grove faults split north of Mineral Hot Springs (Hinkle, 1993). Soil gases over a fault identified by Zohdy and Bisdorf (1993) south of Mineral Hot Springs also had exceptionally high concentrations of N_2 and O_2. The reason for the occurrence of high N_2 concentrations over faults is not known, but might be related to ammonium-bearing minerals deposited by hydrothermal solutions. Ammonium-bearing mica, ammonium-feldspar (buddingtonite), and ammonioalunite have been detected in faults and fractures at Hg/Au-bearing hot spring localities in the western United States. Small amounts of both N_2 and NH_3 are present in many geothermal gases. The ammonium in the hydrothermal fluids probably is derived from organic matter in sediments or sedimentary rocks within the hydrothermal system. These ammonium-bearing minerals are stable in the surface environment, however, the stability of the minerals depends on oxygen concentration and pH (Krohn et al., 1988; Ridgeway and Appleton, 1990). Both O_2 concentration and pH would vary considerably within an open fault in a weathering environment. Very high concentrations of N_2 in soil gases might also exist over boiling geothermal fluids. On boiling, much of the N_2 moves preferentially into the steam phase, whereas smaller amounts of NH_3 stay in the liquid phase (Henley et al., 1984). However, although geothermal steam might account for exceptionally high N_2 concentrations in the Noland fault area, it does not account for the accompanying high O_2 concentrations.

A few anomalous sites are located over east-west trending faults detected in the subsurface by resistivity soundings south of the town of Villa Grove and south of Mineral Hot Springs (Zohdy and Bisdorf, 1993). The faults are concealed by different amounts of alluvium---the fault south of Mineral Hot Springs is at about 500 m depth, whereas the fault south of Villa Grove is at about 1000 m depth. However, concentrations of N_2 and O_2 are not higher over the 500 m depth fault than over the 1000 m depth fault.

Acid alteration along faults: Sites with >95th percentile H+ concentrations (200 ppb H+ or below pH 6.7) represent acid alteration along faults containing sulfide mineralization (fig. 4). A few sites are located over the Sangre de Cristo fault, over faults south of Villa Grove identified by Zohdy and Bisdorf (1993) and on the north side of the eastern anticline. The largest group of samples with anomalous concentrations are located primarily over the Kerber fault. The combination of partially-extracted Zn, Cu, Pb, and Cd, along with high H^+ (figs. 3, 4, and 7) indicates that elements from oxidizing sulfide mineralization have been dissolved, transported upward by water along faults, and adsorbed on clays and Fe and Mn oxides, a situation similar to that at the Roosevelt Hot Springs KGRA, in which high concentrations of several elements were found associated with oxides in fault zones within the geothermal field (Christensen et al., 1983; Hinkle and Copp, in press). The presence of Hg could indicate the possibility of geothermal fluids.

Mo and Cu sulfide mineralization: Several sites with >95th percentile concentrations of Mo and Cu (table 3) are located primarily in drainages in the southeastern part of the study area, mostly south of the Orient Mine area to the vicinity of Cotton Creek (fig. 7). Hydrogen-ion contents of many soil samples also were higher than

average in this area, indicating the probability of weathering sulfide minerals. Concentrations of partially-extracted Mo are especially high at the mouth of Garner Creek and sites downstream. Some of the Mo anomalies could be due to weathering detrital Mo sulfides, other anomalies could be due to Mo that was dissolved, transported, and adsorbed on clays and oxides.

The anomalous Mo-Cu sites lie just west of an area identified as anomalous in Mo (Zimbelman, 1989); the Mo probably is derived from the Rito Alto stock in the Sangre de Cristo Mountains about 5 km east of the Orient Mine. Hydrothermal fluids may have deposited sulfide minerals from Garner Creek south to Major Creek along the Sangre de Cristo fault. Alternatively, the fluids may have deposited sulfide minerals in carbonate rocks upslope from the sample sites. Heat sources driving the hydrothermal fluids probably were the Rito Alto stock or possibly an unexposed stock indicated by a contact-metamorphic aureole near the mouth of Garner Creek (Lindsey et al., 1985).

Ag and Hg in sinter deposits: Silver and Hg appear to have been deposited in sinters at the Valley View Hot Springs by geothermal fluids (probably mixed with groundwater) rising through the the Sangre de Cristo fault (fig. 6-7). However, the Ag anomalies downslope from the Orient Mine probably originated from minerals deposited in faults by hydrothermal fluids from the Rito Alto stock about 5 km east of the mine. Other anomalous samples are located along the Kerber and Noland faults and within the Kerber Creek-Major Creek fault zone, and also near faults west of the town of Villa Grove. The low hydrogen-ion content of soils at these sites indicates the absence of acid alteration associated with the deposition---unlike the Mo and Cu along the Sangre de Cristo fault where the hydrogen-ion concentration in soils was high, indicating acid alteration.

Faults permeable to gases: Helium probably is rising through permeable faults. Plots show highest He concentrations located over major faults (fig. 6).

Anomalies near Villa Grove and contamination from Bonanza mines

Several samples south of Villa Grove were anomalous in partially-extracted Cu, Pb, Zn, Cd, and Ag (figs. 3, 4, and 7). These elements might be related to hot brines rising along the fault identified by Zohdy and Bisdorf (1993). However, the sample sites lie within the Kerber Creek floodplain, therefore, the anomalous elements are more likely related to abandoned mines of the Bonanza mining district about 25 km west of Villa Grove. The Kerber Creek floodplain has been severely impacted by base metals from mine drainage and breeched tailings ponds from the Bonanza area (Kirkham and Holm, 1989). Tidball et al. (1994) found high concentrations of Ag, Cu, Pb, Zn, As, Sb, and Sn in Kerber Creek and San Luis Creek stream sediment samples collected during the National Uranium Resource Evaluation (NURE) program. Kerber Creek normally joins San Luis Creek northeast of Villa Grove, but, during periods of high water, some water from Kerber Creek crosses the fields south of town and could deposit metals there. Soil samples collected by Tidball et al. (1995) in the vicinity of Villa Grove also contained high concentrations of Cu, Pb, Zn, As, and other metals.

To help distinguish the sources of the metallic anomalies south of Villa Grove, 62 of the soil samples that were collected near the town were analyzed for 32 elements (total-element analysis) by direct-current arc-emission spectrography

(Grimes and Marrinzino (1968) (appendix A). These samples were collected along the gravelled county road south of Villa Grove and westward along the road toward Bonanza. The samples along the Bonanza road were above the flood level of Kerber Creek and consisted of locally derived materials.

A file was prepared combining the total-element content of the samples as determined by emission spectrography, the content of eight elements as determined by partial-extraction analyses, and the soil-gas concentrations (table 5). Anomalous concentrations (>95th percentiles) of multiple elements were present in samples from several sites, especially those south of Villa Grove. These samples consist of mixtures of elements derived from weathering of different rock types from different localities. In order to determine the sources of the anomalous elements it was first necessary to separate the mixture into groups of elements that could be associated with minerals or rocks.

For statistical analysis, the variables xSb, Ag, and Zn were deleted from table 5, because the majority of measurements were below the lowest level of determination ("L" values). Analytical values listed as "L" for the other variables were converted to real numbers by arbitrarily multiplying the lowest detectable value by 0.1. Correlation coefficients for the file of unqualified and replaced "L" values indicated strong relationships ($r \geq .50$) between several of the variables (table 6). This data set was examined by R-mode factor analysis (Grundy and Miesch, 1987) in order to clarify the element associations and determine suites of elements associated by geology or geochemistry. This method reduces a large number of chemical variables to fewer, more readily explainable relationships.

A six-factor model made the best sense for the purose of identifying the sources of geochemical suites in the data set (table 7). The varimax loadings in table 7 are arranged in descending order. Loadings greater than $\pm$ 0.5 represent strong positive or negative correlations of the variables with the factor. Most of the factors were related to minerals in sediments carried by Kerber Creek and deposited on fields south of Villa Grove.

The six-factor model was chosen for illustration of the anomaly sources, however, these actually were the first six factors of a nine-factor model that explained more element variances (tables 8-9) because it identified additional mineralogy of the bedrock. The elements in factors 2, 3, and 5 of the six-factor model and factors 2, 3, 5, 7, 8, and 9 in the nine-factor model are derived from minerals in Precambrian granite and Tertiary volcanic bedrock west of Villa Grove.

Factor scores were calculated for each sample in the six-factor model. The factor score expresses the degree of similarity between the factor composition and the composition of a sample. Each factor in a sample has a score (Tidball et al., 1986). The scores may be positive or negative, depending on the composition of the sample. Sample scores above the 95th percentile were used to plot the distribution of factors (fig. 9), and to illustrate the sources of the anomalies south of Villa Grove.

The factor-1 elements Cu, Pb, Zn, Ag, and Mo are derived from sulfide minerals in mine dumps at Bonanza. The total element contents of factor-1 represent detrital minerals deposited on the fields by Kerber Creek. The partially-extracted metal contents of factor-1 are derived from weathering of these detrital minerals and also

from metals dissolved from sulfides at Bonanza by acid mine drainage and transported downstream to the fields south of Villa Grove.

Factor-2 consists of Fe, V, Ti, and other elements from detrital Precambrian granitic rocks and Tertiary volcanics west of Villa Grove, and their weathering products. The negative loadings for Ca and xAs in factor-2 indicate the absence of carbonate rocks containing As mineralization.

Factor-3 consists of Be, B, Sc, La, and Sr, probably associated with tourmaline and beryl from pegmatites weathering from Precambrian bedrock in the hills about five km west-northwest of Villa Grove (Burbank and Henderson, 1932; Bridwell, 1968; Knepper, 1974). The negative hydrogen-ion loading indicates that soils at these sites are alkaline.

Factor-4 consists of N_2, O_2, and CO_2 rising from concealed northwest-trending faults west of Villa Grove and over the east-west faults south of Villa Grove identified by Zohdy and Bisdorf (1993). The high positive loadings indicate that the ground is permeable to gases at these sites. The negative Hg and P indicates the absence of minerals containing these elements. The anomalous soil gases of factor-4 are the only variables that definitely are unrelated to contamination, and appear to be related solely to the concealed faults south of Villa Grove and the major faults west of the town.

Factor-5 consists of elements weathered from feldspars, barite, and other minerals in the Precambrian bedrock west-northwest of Villa Grove. Helium in soil gases is low at the anomalous factor-5 sites, indicating that the ground is impermeable to gases rising from below.

The factor-6 elements As, Sr, and Ca probably are related to sulfide mineralization in carbonate rocks exposed along the Bonanza road about six km west of Villa Grove. Factor-6 elements also could be related to old hot-spring deposits or to detrital sulfide minerals from the eastern anticline area (Burbank and Henderson, 1932; Bridwell, 1968; Knepper, 1974).

DISCUSSION--BIOGEOCHEMISTRY

Relationship of soil and soil-gas factors to biogeochemistry

Both Li and B in plants are excellent indicators of leakage of fluids and gases from geothermal sources to the ground surface. Brown (1981) reported that, of 26 elements examined in controlled plant/root media experiments, Li was the best indicator of geothermal contamination. Soluble Li in soils is readily available to plants perhaps because it appears to share the K^+ transport carrier and is therefore easily translocated. Boron uptake by plants is more highly correlated with its concentration in the nutrient solution (or substrate) than most other elements, including Li (Kabata-Pendias and Pendias, 1984). Anomalous concentrations of these two elements in rabbitbrush occur most notably south of Mineral Hot Springs, at the same sites where soil and soil-gas concentrations are also anomalous (fig. 10). These anomalous plants, soils, and soil-gases are located directly over inferred east-west faults in the subsurface that are related to the geothermal system at Mineral Hot Springs (Zohdy and Bisdorf, 1993).

Rabbitbrush south of Mineral Hot Springs also contains anomalous concentrations of Mn and Fe. Both Mn and Fe oxides in soils over subsurface faults of this area would serve as adsorbants and concentrate Cu, Pb, Zn, Cd, and Hg near Mineral Hot Springs. Anomalous concentrations of Fe in rabbitbrush along the Sangre de Cristo fault and Villa Grove fault zone probably are derived from pyrite and iron oxides associated with Mo and Cu sulfide mineralization within the faults, which acted as passageways for fluids from the Rito Alto stock.

Rabbitbrush sampled along the Sangre de Cristo fault south and in the valley southwest of Valley View Hot Springs also contained very high concentrations of Br that have no easily-identified source. Marine limestones of the Minturn Formation, are a possible source; although these rocks are considerably downdropped by the Sangre de Cristo fault (Lindsey and Soulliere, 1987), bromine dissolved from bedrock by upwelling groundwaters would be available to plants along the Kerber Creek-Major Creek fault zone. Another possible source of Br in rabbitbrush is lacustrine clays and unconsolidated sands of the Neogene Alamosa Formation, which lies just below the alluvial fans (Huntley, 1979). A third source of Br could be organic matter in the Alamosa Formation or oil seeps in the underlying rocks. In 1994, oil was discovered in Cretaceous sediments about 17 km south of the area of Br anomalies. Drill hole data from the oil discovery area indicate that Mesozoic sediments comprise the hanging wall of a low-angle, detachment-syle fault located between the mountain front and the San Luis basin (Watkins et al., 1995).

Anomalies of Zn and Cd occur in both soil and rabbitbrush on the eastern sides of the eastern anticline, near a breccia hill and northwesterly-trending fault that passes through the Mineral Hot Springs area. The Zn and Cd may be adsorbed on Fe and Mn oxides which are also anomalous in the area (Erdman et al., 1993).

Possible indicator value of the plants *Eriogonum Effusum and Erotia Lanata*

Cannon (1971) found that species of *Eriogonum*, a genus in the buckwheat family, "are particularly common on gypsiferous soils and on soils derived from sulfide deposits." Billings (1950, p. 67) may have been the first to associate *E. wriightii*, a species similar to *E. effusum*, with chemically altered rocks. He found mats of that species in transition zones between altered and unaltered andesites in the Virginia Mountains near Reno, Nevada. Recently, Erdman et al. (in press) described the unusual dominance of *E. ovalifolium* growing in silver-laden soils in the Lava Creek mining district of Idaho. Other studies have documented the association of species in this genus with mineralized terrain (Erdman, unpublished data). Although these species commonly occur on sulfur- or sulfate-rich soils, as Chaffee (1975) cautions, "Unfortunately, these species do not differentiate between biogenic-sedimentary sulfide and sulfate concentrations, and hydrothermally-introduced sulfide and sulfate concentrations." The fact remains that some species in the genus *Eriogonum* tend to indicate sulfur-rich substrates, and the results of our study point to specific areas where *E. effusum* is unusually dominant in parts of this landscape.

Sites where this species was found are found just west of the Sangre de Cristo range-front fault and south of its juncture with the younger Villa Grove fault zone where anomalous concentrations of Mo and Cu in soils are found. Another cluster of sites where this species was observed lies generally east of Claytor Cone, in the eastern anticline area near Kerber Creek.

However, the sites associated with the traverse that leads towards Steel Canyon across the Villa Grove fault zone drew our greatest interest. On a conspicuous fault scarp at the center of the traverse, large silicified boulders (some of which had epidote-coated slickensides) were exposed at the surface (fig. 11). Epidote is an aluminum-iron silicate mineral. Prospect pits were also common on the scarp. Along this traverse we found geochemical anomalies in the rabbitbrush sampled and to some extent in the associated soils. The rabbitbrush biogeochemical "signature" shows (i) a strong aluminum-iron-titanium outlier (Erdman and Van Trump, 1993, table 3) that might have resulted from the alteration and leakage through the fault of the minerals sphene or rutile, (ii) a light rare-earth-element suite that had a similar source, and (iii) bromine and lithium anomalies that at least, in part, appear to indicate leakage of brines.

The appearance of stressed Eriogonum and the occurrence of winterfat, Eurotia lanata (Pursh) Moq., a halophyte or plant that indicates saline conditions, further upport the geochemical evidence that this locality is extremely anomalous. The observation of yellowed *Eriogonum* is significant in that such yellowing (chlorosis) can be caused by an aluminum-induced iron deficiency (Kabata-Pendias and Pendias, 1984). The occurrence of winterfat along the fault scarp is not usual—a condition called "out-of-context." Winterfat and other halophytes, such as greasewood (*Sarcobatus vermiculatus* [Hook.] Torr.), more commonly occur either where conditions are clearly alkaline-saline at the center of the San Luis Valley or along the western margin.

CONCLUSIONS

Surficial soil, soil-gas, and plant surveys indicated that the geothermal field of Mineral Hot Springs may be more extensive than the area of the surface springs. Surface expression of the geothermal field for Valley View Hot Springs, on the other hand, is much more restricted, perhaps because the heat source may lie in the foothills of the Sangre de Cristo Range and east of the bounding fault.
R-mode factor analysis of soil and soil-gas data suggests six causes of geochemical anomalies (table 3): (1) epithermal mineralization in carbonate bedrock in the eastern anticline area, (2) fossil or present-day geothermal activity with accompanying hot-spring deposition along the Kerber and Noland faults, the Kerber Creek-Major Creek fault zone, the area north of Mineral Hot Springs where the Noland, Clayton, and Villa Grove faults split, the Sangre de Cristo fault, and the hills of the eastern anticline (3) acid alteration along faults containing sulfide mineralization primarily over the Kerber fault, the eastern anticline area, and over faults south of Villa Grove identified by Zohdy and Bisdorf (1993) (4) Mo and Cu sulfide mineralization, probably are related to the Rito Alto stock, in drainages along the mountain front from the Orient Mine area to the vicinity of Cotton Creek, (5) hot-spring sinter deposition of Ag and Hg at Valley View Hot Springs, along the Kerber and Noland faults, and within the Kerber Creek-Major Creek fault zone, and (6) He rising through permeable faults.

Soil, soil-gas, and plant data indicate the presence of epithermal mineraliztion or of a possible geothermal heat source along the Kerber and Noland faults west and northwest of Mineral Hot Springs. A large cluster of the geothermal indicator elements He, CO_2, and Hg in this area indicate probable fossil hot-spring activity. Above average concentrations of N_2 and O_2 along the Noland fault might indicate active degassing of geothermal fluids.

Anomalies of He, CO_2, and Hg are also located around the hills of the eastern anticline area. Arsenic and Sb anomalies in the same area indicate fossil hot-spring deposits, epithermal mineralization in carbonate bedrock, or both.

Many of the anomalies determined by the geochemical and biogeochemical surveys were related to faults and fault zones that could be identified on the surface. Other anomalies detected subsurface faults concealed by alluvium. For example, factor-1 (geothermal activity and hot-spring deposits) anomalies in soil and soil-gas samples and anomalies of Li and B in rabbitbrush were located directly over concealed east-west faults south of Mineral Hot Springs detected earlier by a resistivity survey (Zohdy and Bisdorf, 1993). The areal agreement of geochemical anomalies in surficial samples with subsurface faults detected by a resistivity survey was a significant result of the integrated studies.

ACKNOWLEDGEMENTS

This work was funded by the U.S. Department of Energy, Geothermal Technology Division. Voucher specimen (a specimen that has been retained to provide proof of identification) samples of the two species of rabbitbrush collected were confirmed by Dr. Loran C. Anderson, Florida State University, Tallahassee, a leading authority on the genus Chrysothamnus. Tom Hopkins, USGS, analyzed the Villa Grove area samples by emission spectrography. Steve Sutley, USGS, used X-ray analysis to identify epidote in the mineral coating on slickenslides. We thank the many ranchers who permitted us to collect samples on their property.

REFERENCES

Barrett, J.K., and Pearl, R.H., 1976, Hydrogeological data of thermal springs and wells in Colorado: Colo. Geol. Surv., Dept. of Nat. Resources, Information Series No. 6, 114 p.

Barrett, J.K., and Pearl, R.H., 1978, An appraisal of Colorado's geothermal resources: Colo. Geol. Surv., Dept. of Natural Resources, Bull. 39, 224 p.

Billings, W.D., 1950, Vegetation and plant growth as affected by chemicaly altered rocks in the western Great Basin: Ecology, vol. 31, p. 62-74.

Bridwell, R.J., 1968, Geology of the Kerber Creek area, Saguache County, Colorado: M.S. thesis, no. 1177, Colo. School of Mines, 104 p.

Brown, K.W., 1981, Geothermal environmental assessment--Behavior of selected geothermal brine contaminants in plants and soils: Sci. of the Total Environment, v. 22, p. 61-77.

Burbank, W.S., and Goddard, E.N., 1937, Thrusting in Huerfano Park, Colorado, and related problems of orogeny in the Sangre de Cristo Mountains: Bull. of the Geol. Soc. of America, v. 48, p. 931-976.

Burbank, W.S., and Henderson, C.W., 1932, Geology and ore deposits of the Bonanza Mining District, Colorado: U.S. Geol. Surv. Prof. Paper 169 p.

Cannon, H.L., 1971, The use of plant indicators in ground water surveys, geologic mapping, and mineral prospecting: Taxon, vol. 20, p. 227-256.

Chaffee, M.A., 1975, Geochemical exploration techniques applicable in the search for copper deposits: U.S. Geol. Surv. Prof. Paper 907-B, 26 p.

Christensen, O.D., Capuano, R.A., and Moore, J.N., 1983, Trace-element distribution in an active hydrothermal system, Roosevelt Hot springs Thermal Area, Utah: J. Volcanology and Geothermal Research, v. 16, p. 99-129.

Davis, T.L., and Stoughton, Dean, 1979, Rio Grande Rift: Tectonics and magmatism, in Riecker, R.E., ed., Am. Geophys. Union, p. 185-194.

Dixon, 1989, Relationships of the greasewood community to groundwater in the San Luis Valley, in Colorado Ground-Water Association, Water in the Valley, Eighth Ann. Field Trip, p. 169-176.

Doesken, N.J., and McKee, T.B., 1989, The incredible climate of the San Luis Valley, in Water in the valley---A 1989 perspective on water supplies, issues, and solutions in the San Luis Valley, Colorado: Colo. Ground-Water Assn. Guidebook, 8th Annual Field Trip, August 19-20, 1989, p. 80-98.

Erdman, J.A., Hinkle, M.E. Watson, Ken, Gallagher, A.J., Ager, C.M., and Smith, K.S., 1993, A new approach to geothermal exploration--integrating geochemistry with remote sensing [Abs.]: The 16th Int. Geochem. Exploration Symp., Beijing, China, p. 40-41.

Erdman, J.A., Moye, Falma, Skipp, Betty, and Theobald, P.K., in press, Geochemical evidence of epithermal metallization in Missippian turbidites of the McGowan Creek Formation, Lava Creek district, Idado, in Worl, R.G., et al., eds., Geology and mineral resources of the Hailey and western Idaho Falls quadrangles, Idaho: U.S. Geol. Surv. Bull. 2064-O.

Erdman, J.A., and VanTrump, George, 1993, Analytical results, basic statistics, and locality map of rabbitbrush (genus *Chrysothamnus*) samples from the Mineral Hot Springs and Valley View Hot Springs Known Geothermal Resource Areas, northern San Luis Valley, Colorado: U.S. Geol. Surv. Open-File Rep. 93-17, 18 p.

Grimes, D.J., and Marranzino, A.P., 1968, Direct-current arc and alternating-current spark emission spectrographic field methods for the semiquantitative analysis of geologic materials: U.S. Geol. Surv. Circ. 591, 6 p.

Grundy, W.D., and Miesch, A.T., 1987, Brief descriptions of STATPAC and related statistical programs for the IBM Personal Computer: U.S. Geol. Surv. Open-File Rep. OF-87-411-A, 34 p.

Henley, R.W., Truesdell, A.H., Barton, P.B., Jr., and Whitney, J.A., 1984, Fluid-mineral equilibria in hydrothermal systems, in Robertson, J.M., ed., Society of Economic Geologists,Reviews in Econ. Geol., v. 1, p. 45-56.

Hinkle, M.E., 1993, Concentrations off N_2, O_2, CO_2, and He in soil gases collected in the northern San Luis Valley, Colorado: U.S. Geol. Surv. Open-File Rep. 93-584, 16 p.

Hinkle, M.E., and Copp, J.F.,in press, Soil and soil-gas geochemistry over and near the Roosevelt Hot Springs KGRA, Utah: accepted by the Journal of Applied Geochemistry.

Huntley, D., 1979, Ground-water recharge to the aquifers of northern San Luis Valley, Colorado: Summary: Geol. Soc. of America Bull., part I, v. 90, p. 707-709.

Johnson, B.R., Lindsey, D.A., Ellis, C.E., Hannigan, B.J., and Thompson, J.R., 1984a, Mineral resource potential of the Sangre de Cristo Wilderness Study Area,sourth-central Colorado: U.S. Geol. Surv. Misc. Field Studies Map MF-1635A.

Johnson, B.R., Lindsey, D.A., Bruce, R.M., and Soulliere, S.J., 1984b, Reconnaissance geologic map of the Sangre de Cristo Wilderness Study Area, south-central Colorado: U.S. Geol. Surv. Misc. Field Studies Map MF-1635B.

Kabata-Pendias, A., and Pendias, H., 1984, Trace elements in soils and plants: CRC Press, Inc., Boca Raton, Florida, 315 p.

Kirkham, R.M., and Holm, J.D., 1989, Environmental problems and reclamation activities at inactive metal mine and milling sites in San Luis Valley, in Water in the Valley: Colo. Ground-Water Assn., 8th Annual Field Trip, August 19-20, 1989, p. 209-227.

Knepper, D.H., Jr., 1974, Tectonic analysis of the Rio Grande Rift Zone, central Colorado: PhD thesis, no. 1593, Colo. School of Mines, 237 p.

Knepper, D.H., Jr., 1976, Late Cenozoic structure of the Rio Grande Rift zone, central Colorado in Epis, R.C., and Weimer, R.J., Studies in Colorado field geology, Colo. School of Mines Prof. Contrib., no. 8, p. 421-430.

Knepper, D.H., Jr., and Marrs, R.W., 1971, Geological development of the Bonanza-San Luis Valley-Sangre de Cristo Range area, south-central Colorado, in James, H.L., Guidebook of the San Luis Basin, Colorado: New Mexico Geol. Soc., twenty-second field conf., p. 249-264.

Krohn, M.D., Altaner, S.P., and Hayba, D.O., 1988, Distribution of ammonium minerals at Hg/Au-bearing hot springs deposits: initial evidence from near-infrared spectral properties, in Schafer, R.W., Cooper, J.J., and Vikre, P.G., eds., Bulk mineable precious metal deposits of the western United States, Geol. Soc. of Nevada Symp. Proc., Reno, NV, p. 661-679.

Lindsey, D.A., Johnson, B.R., and Andriessen, P.A.M., 1983, Laramide and Neogene structure of the northern Sangre de Cristo Range, south-central Colorado, in

Lindsey, D.A., and Soulliere, S.J., 1987, Geologic map and sections of the Valley View Hot Springs Quadrangle, Custer and Saguache Counties, Colorado: U.S. Geol. Surv. Misc. Field Studies Map MF-1942.

Lowell, J., ed., Rocky Mountain foreland basins and uplifts: Rocky Mountain Assn. of Geologists, Symp., Denver, Colorado, p. 219-228.

Motooka, J.M., O'Leary, R.M., Fey, D.L., and Hinkle, M.E., 1994, Analytical results for soil samples collected in the northern San Luis Valley, Colorado: U.S. Geol. Surv. Open-File Rep. 94-297, 25 p.

Ridgeway, J., and Appleton, J.D., 1990, Ammonium geochemistry in mineral exploration--a comparison of results from the American cordillas and the southwest Pacific: Appl. Geochem., v. 5, no. 4, p. 475-489.

Scott, G.R., Taylor, R.B., Epis, R.C., and Wobus, R.A., 1978, Geologic map of the Pueblo 1^0 x 2^0 quadrangle, south-central Colorado: U.S. Geol. Surv. Misc. Investigations Series, Map I-1022.

Selner, G.I., and Taylor, R.B., 1992, System 8. Programs to assist workers in the earth sciences in using geodetic or cartesian xyz data from row column (GSPV85) files: GSPDC, contours and grids interpolated from triangulated network; GSPCS, graphic sections; GSPIV, univariant statistics and histograms; GSPPROB, probability diagrams; GSPXY, regression statistics and XY plots; GSPTD, ternary diagrams, and GSPV85, postplots, for IBM PC and compatible computers: U.S. Geol. Surv. Open-File Rep. 92-372, 83 p.

Swanberg, C.A., 1979, Chemistry of thermal and nonthermal groundwaters in the Rio Grande Rift and adjacent tectonics provinces, in Reicker, R.E., ed., Rio Grande Rift: Tectonics and Magmatism, p. 279-288.

Tidball, R.R., Severson, R.D., Gent, C.A., and Riddle, G.O., 1986, Element associations in soils of the San Joaquin Valley, California: U.S. Geol. Surv. Open-File Rep. 86-583, 15 p.

Tidball, R.R., Stewart, K.C., Tripp, R.B., and Mosier, E.L., 1995, Geochemical mapping of surficial materials in the San Luis Valley, Colorado, in Posey, H.H., Pendleton, J.A., and Van Zyl, Dirk, 1995, Proceedings: Summitville Forum '95: Colo. Geol. Surv. Spec. Publication 38, p. 244-262.

Tidball, R.R., Smith, S.M., and Stewart, K.C., 1994, Geochemical mapping in the San Luis Valley, Colorado--hydrogeochemical and stream sediment data (abstract), in Carter, L.M.H., Toth M.I., and Day, W.C., USGS Research on Mineral Resources--1994, part A--program and abstracts, ninth V.E. McKelvey Forum on Mineral and Energy Resources: U.S. Geol. Surv. Circ. 1103-A, p. 105-106.

Tweto, Ogden, Steven, T.A., Hail, W.J., Jr., and Moench, R.H., 1976, Preliminary geologic map of the Montrose 1^0 x 2^0 quandrable, southwestern Colorado: U.S. Geol. Surv. Misc. Field Studies Map MF-761.

Watkins, T., Belcher, J., Gries, R., and Longacre, M., 1995, The surprising discovery of oil and Mesozoic sediments in the San Luis Basin, Saguache County, Colorado (abstract): Colo. Scientific Soc. Newsletter, May, 1995, p.2.

White, D.E., 1970, Geochemistry applied to the discovery, evaluation, and exploitation of geothermal energy resources: Proceedings of the United Nations symposium on the development and utilization of geothermal resources, Pisa, Italy, Geothermics, Special Issue 2, September 22-October 1, 1970, p. 58-80.

Zimbelman, D.R., 1989, Maps showing trace-element geochemistry of the Sangre de Cristo wilderness study area, south-central Colorado: U.S. Geol. Surv. Misc. Field Studies Map MF-1635C.

Zohdy, A.A.R., and Bisdorf, R.J., 1993, A direct-current resistivity survey near Mineral Hot Springs, San Luis Valley, Colorado: U.S. Geol. Surv. Open-File Rep. 93-282, 61 p.

Table 1. Concentrations of elements in spring waters (Barrett and Pearl, 1976)--averaged analyses of 3 springs at each site.

Variable	Mineral Hot Springs	Valley View Hot Springs
As (ug/L)	30	1
B (ug/L)	372	30
Cd (ug/L)	0.5	1
Ca (mg/L)	58	48
Cl (mg/L)	40	1.8
F (mg/L)	4	0.4
Fe (ug/L)	80	20
Li (ug/L)	322	8
Mg (mg/L)	13	14
Mn (ug/L)	20	7
Hg (ug/L)	nd	nd
N (mg/L)	2.1	0.21
phosphate as P (mg/L)	0.03	0.01
phosphate as ortho-P04 (mg/L	0.08	0.03
K (mg/L)	14	2.4
Se (ug/L)	nd	nd
Si02 (mg/L)	48	19
Na (mg/L)	140	3.6
S04 (mg/L)	180	85
Zn (ug/L)	7	5
alkalinity as CaC03 (mg/L)	283	103
alkalinity as HC03 (mg/L)	345	125
non-C03 hardness (mg/L)	nd	76
total hardness (mg/L)	200	176
specific conductance (microm	1014	366
total dissolved solids (mg/L	680	237
pH, field	6.7	6.8
discharge (gallons per minut	108	75
temperature (C)	60	34

nd=not detected

Table 2. Concentrations of elements in sinters (Motooka and others, 1994).

Element	Mineral Hot Springs (1-sample)	Valley View Hot Springs (1-sample)
Al (%)	0.14	0.76
Ca (%)	40	38
Fe (%)	0.55	0.38
K (%)	0.07	0.30
Mg (%)	0.91	0.70
Na (%)	0.06	0.09
P (%)	0.01	0.03
Ti (%)	0.007	0.02
Mn (ppm)	370	120
Ag (ppm)	<2	6
As (ppm)	49	<10
Au (ppm)	<8	<8
Ba (ppm)	240	320
Be (ppm)	6	<1
Bi (ppm)	<10	<10
Cd (ppm)	<2	<2
Ce (ppm)	<4	7
Co (ppm)	2	8
Cr (ppm)	1	6
Cu (ppm)	3	6
Eu (ppm)	<2	<2
Ga (ppm)	<4	<4
Ho (ppm)	<4	<4
La (ppm)	3	5
Li (ppm)	23	3
Mo (ppm)	<2	<2
Nb (ppm)	<4	<4
Nd (ppm)	10	15
Ni (ppm)	<2	7
Pb (ppm)	<4	<4
Sc (ppm)	<2	<2
Sn (ppm)	<5	<5
Sr (ppm)	1400	730
Ta (ppm)	<40	<40
Th (ppm)	<4	<4
U (ppm)	<100	<100
V (ppm)	<2	8
Y (ppm)	<2	3
Yb (ppm)	<1	<1
Zn (ppm)	6	29
Hg (ppm)	0.13	0.07

Table 3. Basic statistics and percentiles for soil samples.

Element	Number Unqualified Values *	Minimum	Maximum	Mean	Standard Deviation	**** 25th	**** 50th	**** 75th	**** Percentiles 90th	**** 95th	**** 97.5th	**** 99th
xAg (ppm)	66	L	3.90	0.23	0.49	L	L	L	0.09	0.14	0.30	0.66
xAs (ppm)	392	L	27.0	2.7	1.8	1.9	2.4	3.1	3.8	4.8	7.9	9.5
xCd (ppm)	279	L	1.10	0.24	0.15	L	0.16	0.26	0.36	0.43	0.51	0.84
xCu (ppm)	396	13	77	24	7	19	22	26	32	36	41	57
xMo (ppm)	396	0.36	5.20	0.92	0.52	0.70	0.82	0.96	1.20	1.45	2.35	4.00
xPb (ppm)	396	5.5	130	21	12	15	18	23	32	41	53	79
xSb (ppm)	30	L	4	1.7	0.89	L	L	L	L	1	2.1	2.75
xZn (ppm)	396	16	290	85	38	55	81	100	140	155	170	215
Hg (ppb)	396	10	80	20	12	10	10	30	40	40	50	60
Hydrogen ion (ppb)	396	1	1995	66	173	10	25	63	126	200	316	1000
" " (pH)		5.7	9.0	7.2		8.0	7.6	7.2	6.9	6.7	6.5	6.0

* = no "L" values

Table 4. Correlation coefficients greater than +/- 0.5 for soil and soil-gas data.

xAg	xAs	xCd	xCu	xMo	xPb	xSb	xZn	Hg	H+	N2	O2	CO2	He	
1.00	--	--	--	--	--	--	--	--	--	--	--	--	--	xAg
	1.00	--	--	--	0.59	0.76	--	--	--	--	--	--	--	xAs
		1.00	--	--	0.55	--	--	--	--	--	--	--	--	xCd
			1.00	--	--	--	--	--	--	--	--	--	--	xCu
				1.00	--	--	--	--	--	--	--	--	--	xMo
					1.00	0.59	0.59	--	--	--	--	--	--	xPb
						1.00	--	--	--	--	--	--	--	xSb
							1.00	--	--	--	--	--	--	xZn
								1.00	--	--	--	--	--	Hg
									1.00	--	--	--	--	H+
										1.00	0.96	0.55	--	N2
											1.00	0.54	--	O2
												1.00	--	CO2
													1.00	He

Table 5. Basic statistics and percentiles for samples near Villa Grove.

Variable	Number Unqualified Values *	Minimum	Maximum	Mean	Standard Deviation	**** Percentes 25th	**** 50th	**** 75th	*** 90th	**** 95th	**** 97.5th	**** 99th
xAg (ppm)**	26	L	0.77	0.18	0.16	L	L	0.10	0.20	0.31	0.46	0.64
xAs (ppm)	62	1.50	6.00	2.60	0.80	2.10	2.50	3.00	3.30	3.95	4.80	5.65
xCd (ppm)	48	L	0.960	0.260	0.190	0.089	0.175	0.280	0.385	0.520	0.840	0.930
xCu (ppm)	62	15	44	21	5	19	21	22	24	28	33	41
xMo (ppm)	62	0.7	1.4	1.0	0.1	0.9	0.9	1.1	1.2	1.2	1.3	1.4
xPb (ppm)	62	15	100	29	14	21	25	32	43	51	59	82
xSb (ppm)	1	L	1.9	-	-	L	L	L	L	L	L	1.9
xZn (ppm)	62	61	290	102	48	77	84	110	145	210	255	280
Hg (ppb)	35	L	50	27	7	L	20	30	30	30	35	45
H+ (ppb)	62	3	282	49	61	8	11	79	122	178	200	241
N2 (%)	61	64.2	77.8	72.2	2.9	70.7	72.5	74.1	75.5	76.1	77.4	77.6
O2 (%)	61	17.1	21.1	19.4	0.8	18.9	19.5	19.9	20.3	20.4	20.7	21.0
CO2 (%)	61	0.10	0.60	0.33	0.1	0.27	0.32	0.37	0.47	0.53	0.57	0.59
He (ppb)	61	5000	5600	5340	120	5264	5348	5390	5516	5560	5600	5600
Ca (%)***	62	0.1	1.5	0.4	0.4	0.2	0.3	0.5	0.9	1.5	1.5	1.5
Fe (%)	62	1.5	3.0	2.3	0.6	2.0	2.0	3.0	3.0	3.0	3.0	3.0
Mg (%)	62	0.2	0.7	0.4	0.1	0.3	0.5	0.5	0.5	0.5	0.7	0.7
Na (%)	62	0.7	2.0	1.3	0.4	1.0	1.5	1.5	1.8	2.0	2.0	2.0
P (%)	15	L	2.0	0.3	0.4	L	L	L	0.2	0.2	0.2	1.1
Ti (%)	62	0.2	0.5	0.3	0.1	0.2	0.3	0.3	0.3	0.4	0.5	0.5
Ag (ppm)	4	L	2.0	0.9	0.7	L	L	L	L	L	0.9	1.5
B (ppm)	46	L	15	10	1	L	10	10	10	10	12.5	15
Ba (ppm)	62	300	1500	798	201	700	700	1000	1000	1000	1000	1250
Be (ppm)	60	L	1.5	1.1	0.2	1.0	1.0	1.0	1.5	1.5	1.5	1.5
Co (ppm)	62	0.1	20.0	12.0	4.0	10.0	10.0	15.0	15.0	17.5	20.0	20.0
Cr (ppm)	62	10	100	43	18	30	50	50	70	70	70	85
Cu (ppm)	62	15	50	24	7	20	20	30	30	30	40	50
Ga (ppm)	62	10	30	22	6	20	20	30	30	30	30	30
La (ppm)	60	L	50	50	0	50	50	50	50	50	50	50
Mn (ppm)	62	300	700	526	122	500	500	600	700	700	700	700
Nb (ppm)	20	L	30	21	2	L	L	20	20	20	20	25
Ni (ppm)	62	15	30	18	3	15	20	20	20	20	20	25
Pb (ppm)	62	20	150	52	33	30	40	70	100	100	150	150
Sc (ppm)	62	5	10	7	1	7	7	7	7	7	7	9
Sr (ppm)	62	100	200	170	28	150	150	200	200	200	200	200
V (ppm)	62	30	100	59	17	50	50	70	70	85	100	100
Y (ppm)	62	15	30	18	3	15	20	20	20	20	20	25
Zn (ppm)	2	L	200	200	0	L	L	L	L	L	L	200
Zr (ppm)	62	70	300	194	73	150	200	300	300	300	300	300

* No "L" (below detection level) values
** Samples with "x" prefix are by ICP analysis
***Remaining samples by spectrography

Table 6. Variables in samples near Villa Grove (correlations) +/- 0.5).

xAg	xAs	xCd	xCu	xMo	xPb	xZn	Hg	H+	N2	02	C02	He	Ca	Fe	Mg	Na	P	Ti	B	Ba	Be	Co	Cr	Cu	Ga	La	Mn	Nb	Ni	Pb	Sc	Sr	V	Y	Zr	
1.00	--	0.75	0.81	--	0.90	0.82	--	--	--	--	--	--	--	--	--	--	--	--	--	--	--	--	--	0.68	--	--	--	--	--	0.62	--	--	--	--	--	xAg
	1.00	--	--	--	--	--	--	--	--	--	--	--	0.64	--	--	--	--	--	--	--	--	--	--	--	--	--	--	--	--	--	--	--	--	--	xAs
		1.00	0.61	0.54	0.85	0.82	--	0.54	--	--	--	--	--	--	--	--	--	--	--	--	--	--	--	0.73	--	--	--	--	--	0.76	--	--	--	--	--	xCd
			1.00	--	0.74	0.70	--	--	--	--	--	--	--	--	--	--	--	--	--	--	--	--	--	0.63	--	--	--	--	--	--	--	--	--	--	--	xCu
				1.00	0.50	--	--	--	--	--	--	--	--	0.50	--	--	--	--	--	--	--	--	--	0.54	--	--	--	--	--	0.57	--	--	0.54	--	--	xMo
					1.00	0.86	--	0.57	--	--	--	--	--	--	--	--	--	--	--	--	--	--	--	0.80	--	--	--	--	--	0.79	--	--	--	--	--	xPb
						1.00	--	--	--	--	--	--	--	--	--	--	--	--	--	--	--	--	--	0.74	--	--	--	--	--	0.71	--	--	--	--	--	xZn
							1.00	--	--	--	--	--	--	--	--	--	--	--	--	--	--	--	--	--	--	--	--	--	--	--	--	--	--	--	--	Hg
								1.00	--	--	--	--	--	--	--	--	--	--	--	--	--	--	--	0.55	--	--	--	--	--	0.61	--	--	0.57	--	0.50	H+
									1.00	0.91	--	--	--	--	--	--	--	--	--	--	--	--	--	--	--	--	--	--	--	--	--	--	--	--	--	N2
										1.00	--	--	--	--	--	--	--	--	--	--	--	--	--	--	--	--	--	--	--	--	--	--	--	--	--	02
											1.00	--	--	--	--	--	--	--	--	--	--	--	--	--	--	--	--	--	--	--	--	--	--	--	--	C02
												1.00	--	--	--	--	--	--	--	--	--	--	--	--	--	--	--	--	--	--	--	--	--	--	--	He
													1.00	--	--	--	--	--	--	--	--	--	--	--	--	--	--	--	--	--	--	--	--	--	--	Ca
														1.00	--	--	--	0.55	--	0.63	--	0.68	--	0.52	--	--	--	--	--	--	--	--	0.69	--	0.57	Fe
															1.00	--	--	--	--	--	--	--	--	--	--	--	--	--	--	--	--	--	--	--	--	Mg
																1.00	--	--	--	0.52	--	--	--	0.67	0.66	--	--	--	--	0.71	--	--	--	--	--	Na
																	1.00	--	--	0.53	--	--	--	--	--	--	--	--	--	--	--	--	--	--	--	P
																		1.00	--	--	--	0.51	--	--	--	--	--	0.52	--	--	--	0.57	--	0.60	Ti
																			1.00	--	--	--	--	--	--	--	--	--	--	--	--	--	--	--	--	B
																				1.00	--	0.58	0.55	0.51	0.62	--	0.51	--	--	0.59	--	--	0.72	--	--	Ba
																					1.00	--	--	--	--	--	--	--	--	--	--	--	--	--	--	Be
																						1.00	--	--	--	--	--	--	--	--	--	0.66	--	--	Co
																							1.00	--	--	--	--	--	--	--	--	--	0.54	--	--	Cr
																								.1.00	.50	--	--	--	--	0.76	--	--	--	--	--	Cu
																									1.00	--	--	--	--	0.59	--	--	--	--	--	Ga
																										1.00	--	--	--	--	--	--	--	--	--	La
																											1.00	--	--	0.50	--	--	--	--	--	Mn
																												1.00	--	--	--	--	0.50	--	Nb
																													.1.00	--	--	--	--	--	Ni
																														1.00	--	--	0.53	--	--	Pb
																															1.00	--	--	--	--	Sc
																																1.00	--	--	--	Sr
																																	1.00	--	0.63	V
																																		1.00	--	Y
																																			1.00	Zr

Table 7. Varimax loadings for the 6-factor model: samples near Villa Grove.

Factor-1		Factor-2		Factor-3		Factor-4		Factor-5		Factor-6	
xAg	0.929	Fe	0.801	Be	0.774	N2	0.890	Mg	0.644	xAs	0.662
xPb	0.917	V	0.766	Sc	0.541	O2	0.826	Ga	0.563	Ca	0.656
xZn	0.877	Ti	0.744	B	0.465	CO2	0.583	Ba	0.548	Sr	0.620
xCu	0.863	Co	0.736	La	0.451	Sr	0.203	Na	0.513	La	0.414
xCd	0.844	Zr	0.710	Y	0.427	Sc	0.197	Pb	0.478	Mi	0.406
Cu	0.778	Ba	0.693	Mg	0.285	Fe	0.146	Mn	0.406	Mg	0.295
Pb	0.663	Nb	0.649	Ni	0.262	Y	0.143	Cu	0.287	Sc	0.227
Hg	0.471	Cr	0.608	Nb	0.219	Ga	0.123	Hg	0.252	P	0.198
xMo	0.458	Y	0.522	xCu	0.159	La	0.120	Cr	0.246	xCu	0.187
H+	0.371	P	0.517	Sr	0.135	Co	0.087	Be	0.241	Cr	0.157
Na	0.351	xMo	0.516	O2	0.128	Cr	0.079	V	0.236	O2	0.145
Fe	0.256	Ga	0.488	Ti	0.126	xAg	0.057	H+	0.157	Ba	0.140
V	0.237	Mn	0.415	Mn	0.107	Nb	0.055	xPb	0.151	N2	0.120
Ga	0.229	H+	0.395	Ga	0.101	Na	0.050	xZn	0.138	He	0.079
Mn	0.215	Na	0.355	Fe	0.051	He	0.046	xCd	0.125	Co	0.035
Mg	0.208	Pb	0.330	xZn	0.037	xZn	0.038	P	0.121	V	0.020
Co	0.202	Cu	0.320	P	0.035	xPb	0.036	xCu	0.111	Mg	0.017
Ba	0.190	Sc	0.286	CO2	0.033	Pb	0.015	Sc	0.095	xAg	0.011
Ti	0.154	xPb	0.228	Cr	0.028	xCu	0.008	O2	0.095	Nb	-0.021
xAs	0.131	xCd	0.224	Ca	0.003	V	-0.007	Ca	0.093	Be	-0.029
N2	0.112	Mg	0.182	N2	0.001	xAs	-0.013	Fe	0.093	xPb	-0.043
B	0.186	CO2	0.166	xAg	-0.003	xMo	-0.027	Co	0.086	Ga	-0.069
O2	0.069	Sr	0.162	He	-0.036	Cu	-0.038	N2	0.072	Fe	-0.070
Cr	0.007	Ni	0.153	Cu	-0.055	Be	-0.038	Zr	0.063	Cu	-0.119
Sc	-0.003	xZn	0.112	Hg	-0.064	Ba	-0.042	Sr	0.016	CO2	-0.125
Be	-0.007	He	0.039	Ba	-0.085	Mg	-0.044	Y	0.010	xMo	-0.155
La	-0.014	La	0.006	xCd	-0.102	xCd	-0.058	xAg	0.002	xZn	-0.167
P	-0.046	xAg	0.000	xAs	-0.111	Ca	-0.068	xHe	-0.019	Pb	-0.190
Zr	-0.047	N2	-0.086	xPb	-0.119	H+	-0.140	xAs	-0.078	Na	-0.200
Nb	-0.121	Be	-0.126	Co	-0.124	Mn	-0.151	Ti	-0.123	xCd	-0.201
He	-0.129	O2	-0.127	Na	-0.139	Ti	-0.151	La	-0.140	Ti	-0.203
Ni	-0.143	B	-0.151	Zr	-0.172	Zr	-0.170	B	-0.273	B	-0.233
CO2	-0.160	xCu	-0.189	Pb	-0.211	Mi	-0.205	CO2	-0.305	Y	-0.243
Sr	-0.172	Hg	-0.214	xMo	-0.225	B	-0.348	Nb	-0.349	Mn	-0.254
Ca	-0.244	Ca	-0.424	V	-0.286	Hg	-0.419	Mi	-0.359	Zr	-0.268
Y	-0.299	xAs	-0.441	H+	-0.566	P	-0.446	He	-0.650	H+	-0.365

Table 8. Varimax loadings for 9-factor model near Villa Grove.

Factor-1		Factor-2		Factor-3		Factor-4		Factor-5		Factor-6		Factor-7		Factor-8		Factor-9	
xAg	0.935	Fe	0.797	Be	0.834	N2	0.916	Mg	0.583	Sr	0.702	B	0.852	Sc	0.664	Na	0.610
xPb	0.930	V	0.761	La	0.620	O2	0.903	Mn	0.465	xAs	0.673	Ni	0.280	Ni	0.582	Ga	0.558
xZn	0.896	Ti	0.755	Sc	0.409	CO2	0.480	Hg	0.436	Ca	0.671	Mn	0.264	Cr	0.523	Cr	0.474
xCd	0.851	Zr	0.741	Sr	0.361	Sc	0.193	Ca	0.277	P	0.354	Be	0.239	Nb	0.335	Ba	0.446
xCu	0.849	Co	0.724	Y	0.304	Sr	0.166	xCu	0.209	Mg	0.328	Y	0.238	La	0.318	Pb	0.404
Cu	0.773	Ba	0.678	Mg	0.252	Y	0.164	Ba	0.169	Ni	0.274	Nb	0.233	xCu	0.190	Mg	0.337
Pb	0.682	Mn	0.589	P	0.141	Mg	0.135	Cu	0.151	La	0.177	Ti	0.204	xAs	0.179	H+	0.272
xMo	0.448	Y	0.572	xZn	0.135	Fe	0.120	Pb	0.146	Ba	0.163	Hg	0.180	Fe	0.134	Cu	0.269
Hg	0.446	Nb	0.509	Ga	0.126	Ga	0.117	Ga	0.128	O2	0.129	xMo	0.126	Co	0.124	P	0.244
H+	0.397	xMo	0.487	xCu	0.109	xCu	0.084	Sc	0.113	xCu	0.099	xAs	0.073	N2	0.093	Be	0.187
Na	0.355	Ga	0.471	CO2	0.086	xAs	0.082	V	0.102	N2	0.045	CO2	0.067	V	0.076	Mn	0.161
Fe	0.258	P	0.454	B	0.079	Ca	0.063	xZn	0.092	CO2	0.039	Mg	0.062	Y	0.076	xMo	0.157
V	0.255	Cr	0.441	Ba	0.058	Na	0.060	Be	0.066	xAg	0.033	xCu	0.042	Hg	0.075	xPb	0.154
Ga	0.239	H+	0.385	O2	0.054	Mo	0.053	xCd	0.061	He	0.026	Cu	0.032	Mg	0.075	Hg	0.138
Co	0.224	Pb	0.378	Nb	0.041	xAg	0.039	Na	0.054	Hg	0.024	xCd	0.024	Ga	0.072	V	0.126
Ba	0.215	Na	0.337	Ti	0.035	xZn	0.035	xAs	0.011	Nb	0.004	P	0.022	Cu	0.064	Fe	0.101
Mn	0.189	Cu	0.324	xAg	0.022	Cr	0.031	B	0.010	Cr	0.003	He	0.015	Ca	0.053	xCd	0.088
Mg	0.184	Mg	0.286	Fe	0.015	Mn	0.030	Ni	0.010	xPb	0.000	Ca	0.014	He	0.045	xAg	0.064
Ti	0.154	xCd	0.255	Ca	0.011	Pb	0.020	Co	0.006	V	-0.004	xAg	0.011	O2	0.044	Zr	0.060
xAs	0.094	xPb	0.210	Mn	-0.023	xPb	0.016	Zr	0.004	Be	-0.007	O2	0.005	B	0.042	Sc	0.058
N2	0.084	Sc	0.195	Co	-0.036	Cu	0.011	O2	0.001	xMo	-0.012	Na	-0.007	Ti	0.030	Nb	0.054
B	0.046	Sr	0.172	Ni	-0.042	Co	0.010	xPb	-0.014	B	-0.029	Zr	-0.008	Ba	0.028	N2	0.049
O2	0.031	xZn	0.172	N2	-0.046	xMo	-0.020	N2	-0.067	Co	-0.035	xZn	-0.037	xAg	0.010	O2	0.035
La	0.019	CO2	0.155	xPb	-0.062	La	-0.025	Y	-0.068	Pb	-0.039	Fe	-0.051	xMo	0.008	Y	0.033
Be	0.008	He	0.103	He	-0.083	Be	-0.026	Fe	-0.074	Fe	-0.048	xPb	-0.083	xPb	-0.037	xCu	0.014
Cr	0.001	Ni	0.084	xCd	-0.092	Nb	-0.026	He	-0.090	Ga	-0.062	Sc	-0.090	P	-0.040	xZn	0.005
Sc	-0.015	xAg	-0.038	Cr	-0.097	xCd	-0.044	xAg	-0.100	Ti	-0.075	Ga	-0.104	Be	-0.042	xAs	-0.008
P	-0.020	N2	-0.071	Pb	-0.099	V	-0.055	Sr	-0.103	Mn	-0.082	Pb	-0.108	Zr	-0.045	Co	-0.018
Zr	-0.040	O2	-0.074	Cu	-0.119	Ba	-0.080	Cr	-0.114	Cu	-0.087	Cr	-0.126	Na	-0.073	Ti	-0.031
Nb	-0.131	B	-0.077	Na	-0.150	Ni	-0.096	H+	-0.124	Na	-0.087	N2	-0.130	Sr	-0.091	Ca	-0.067
He	-0.142	Be	-0.089	xAs	-0.176	B	-0.138	P	-0.151	xZn	-0.109	H+	-0.134	xCd	-0.108	CO2	-0.072
CO2	-0.155	La	-0.113	Hg	-0.200	Ti	-0.161	Ti	-0.173	Sc	-0.116	Sr	-0.189	Mn	-0.150	Sr	-0.099
Sr	-0.159	Hg	-0.176	V	-0.208	Zr	-0.185	xMo	-0.178	xCd	-0.120	La	-0.257	xZn	-0.178	B	-0.121
Ni	-0.194	xCu	-0.195	Zr	-0.208	H+	-0.212	La	-0.206	Zr	-0.176	Ba	-0.298	CO2	-0.229	La	-0.131
Ca	-0.275	Ca	-0.394	xMo	-0.335	Hg	-0.263	Nb	-0.557	H+	-0.188	Co	-0.320	Pb	-0.262	Ni	-0.275
Y	-0.310	xAs	-0.587	H+	-0.481	P	-0.507	CO2	-0.580	Y	-0.197	V	-0.329	H+	-0.303	He	-0.785

Table 9. Percent of variance explained for variables in 6- and 9-factor models.

Variable	6-Factor Model	9-Factor Model
xAg	86	90
xAs	72	81
xCd	82	82
xCu	83	87
xMo	54	59
xPb	92	94
xZn	87	90
Hg	48	64
H+	80	82
N2	80	83
O2	70	77
CO2	51	68
He	41	65
Ca	62	74
Fe	74	75
Mg	64	72
Na	55	63
P	68	85
Ti	67	70
B	52	76
Ba	84	87
Be	61	78
Co	58	67
Cr	48	58
Cu	81	82
Ga	62	63
La	39	65
Mn	53	71
Nb	62	76
Ni	35	63
Pb	85	80
Sc	44	67
Sr	46	63
V	74	83
Y	59	65
Zr	63	66

Appendix A. Results of analyses of samples near Villa Grove. "L" = not detected at lowest level of determination.

Number	Lat	Long	xAg	xAs	xCd	xCu	xMo	xPb	xSb	xZn	Hg	H+	N2	O2	CO2	He	Ca	Fe	Mg	Na	P
121	38.244	105.946	0.300	1.7	0.240	27	0.71	42	L	230	40	45	71.0	19.0	0.34	5222	0.3	2.0	0.5	1.0	0.2
122	38.244	105.945	0.260	2.5	0.780	28	1.10	50	L	190	50	89	68.8	18.4	0.26	5432	0.2	2.0	0.3	0.7	L
123	38.243	105.943	L	1.6	0.190	21	0.99	26	L	110	20	100	74.9	20.3	0.29	5306	0.2	3.0	0.3	1.5	0.0
124	38.241	105.942	0.770	3.0	0.900	44	1.20	100	L	270	30	200	74.1	19.9	0.24	5096	0.2	3.0	0.5	2.0	L
125	38.240	105.940	0.500	3.1	0.960	38	1.30	64	L	290	30	79	72.6	19.5	0.24	5516	0.2	3.0	0.5	2.0	L
126	38.240	105.938	0.081	2.2	0.330	20	1.10	32	L	100	30	112	71.7	19.3	0.32	5306	0.2	3.0	0.5	2.0	L
127	38.238	105.936	0.140	2.5	0.430	24	1.20	51	L	150	30	71	75.5	20.4	0.27	5306	0.3	3.0	0.7	1.5	L
128	38.237	105.936	0.097	2.1	0.400	19	1.10	38	L	110	30	282	69.4	18.6	0.34	5348	0.1	2.0	0.3	1.5	L
129	38.236	105.935	0.097	3.0	0.130	22	1.40	36	L	100	L	48	73.4	19.8	0.27	5348	0.2	3.0	0.5	1.5	L
130	38.235	105.935	0.250	1.7	0.370	25	0.99	46	L	240	L	56	77.4	20.9	0.47	5306	0.3	3.0	0.5	1.5	0.2
131	38.234	105.934	0.100	1.7	0.270	20	0.96	34	L	140	L	79	76.1	18.8	0.32	5324	0.2	2.0	0.5	1.5	L
132	38.233	105.934	L	1.7	0.170	17	0.90	32	L	110	L	200	73.3	19.7	0.39	5228	0.2	2.0	0.3	1.5	L
133	38.231	105.933	0.100	2.2	0.290	18	1.20	33	L	110	30	178	77.4	19.2	0.33	5360	0.2	3.0	0.3	1.5	L
134	38.230	105.933	0.110	2.5	0.530	21	1.20	44	L	130	30	178	69.7	18.6	0.25	5180	0.3	2.0	0.7	2.0	0.2
135	38.229	105.933	0.070	2.2	0.320	21	1.10	39	L	110	20	79	70.3	18.9	0.34	5288	0.2	3.0	0.5	2.0	0.2
136	38.227	105.933	L	2.6	0.190	18	1.20	34	L	98	20	158	64.3	17.8	0.25	5264	0.3	3.0	0.5	1.5	2.0
137	38.226	105.933	0.100	2.1	0.510	18	0.91	41	L	150	30	79	74.5	20.0	0.48	5180	0.3	3.0	0.5	1.5	0.2
138	38.225	105.933	0.079	1.7	0.260	19	0.93	32	L	120	30	79	72.5	19.6	0.22	5264	0.2	2.0	0.5	1.5	L
139	38.222	105.933	0.071	1.5	0.200	17	0.82	32	L	100	20	126	64.8	17.1	0.29	5348	0.2	3.0	0.3	1.5	0.2
140	38.219	105.933	L	1.7	0.250	19	0.98	29	L	110	20	50	70.9	19.0	0.36	5306	0.3	3.0	0.5	1.5	0.2
141	38.216	105.932	L	1.6	0.088	16	1.10	24	L	85	L	112	70.7	19.2	0.60	5432	0.3	3.0	0.3	1.0	0.2
142	38.213	105.932	0.092	1.8	0.120	15	0.86	25	L	88	L	79	74.7	20.0	0.35	5390	0.2	2.0	0.2	1.5	L
143	38.210	105.932	0.081	2.4	0.320	18	0.95	31	L	130	30	40	67.1	18.0	0.14	5222	0.3	3.0	0.5	2.0	0.2
305	38.252	105.951	0.420	5.3	0.200	28	0.93	54	1.90	120	30	10	75.8	20.2	0.46	5390	0.5	2.0	0.5	1.5	L
306	38.252	105.954	L	6.0	L	22	0.85	22	L	77	L	11	75.3	20.4	0.31	5306	1.5	1.5	0.5	1.0	L
307	38.252	105.956	0.069	2.8	0.099	22	0.98	26	L	79	L	10	71.9	19.2	0.21	5348	0.3	2.0	0.3	0.7	L
308	38.251	105.958	0.080	3.3	0.150	24	0.82	22	L	74	30	9	71.3	19.1	0.21	5306	1.5	1.5	0.5	1.5	L
309	38.251	105.960	0.076	2.7	0.310	22	0.84	27	L	90	30	9	77.8	21.1	0.31	5012	0.3	1.5	0.5	0.7	L
310	38.251	105.962	0.110	3.2	0.190	23	0.84	24	L	83	30	9	64.2	17.2	0.10	5306	0.7	1.5	0.5	1.0	L
311	38.251	105.963	L	2.9	0.200	24	0.91	31	L	87	30	8	73.2	19.8	0.33	5264	0.5	3.0	0.7	1.5	0.2
312	38.250	105.965	L	3.2	0.160	23	0.93	21	L	79	20	8	73.8	19.9	0.39	5216	0.5	2.0	0.5	2.0	L
313	38.250	105.967	L	1.9	L	23	0.87	17	L	75	30	8	71.5	19.4	0.28	5252	0.3	1.5	0.5	1.0	L
314	38.249	105.968	L	2.0	0.180	23	0.88	23	L	83	L	7	71.4	19.3	0.29	5558	0.3	2.0	0.5	1.0	L
315	38.248	105.970	L	3.0	L	23	0.80	15	L	70	30	8	70.4	18.9	0.23	5306	1.5	2.0	0.5	1.0	L
316	38.247	105.971	L	2.0	0.091	20	0.93	22	L	71	L	11	73.2	19.7	0.41	5222	0.3	2.0	0.5	1.5	L
317	38.247	105.973	L	2.6	0.170	21	0.91	25	L	78	L	6	75.0	20.2	0.58	5288	0.7	3.0	0.5	1.5	L
318	38.246	105.975	L	2.6	0.110	22	0.87	22	L	75	L	6	73.1	19.7	0.26	5216	0.7	2.0	0.5	0.7	0.2
319	38.246	105.977	L	2.6	0.180	22	0.98	25	L	79	L	4	67.7	18.1	0.30	5348	0.3	2.0	0.5	1.0	L
320	38.245	105.978	L	2.2	0.091	21	0.93	21	L	75	L	13	74.4	20.1	0.32	5348	0.5	2.0	0.5	1.0	L
321	38.244	105.980	L	2.2	0.120	22	0.96	23	L	79	L	9	72.3	19.4	0.37	5390	0.7	3.0	0.5	1.0	0.2
322	38.244	105.982	L	2.9	L	22	0.85	17	L	65	20	10	72.5	19.6	0.33	5474	0.7	2.0	0.3	0.7	L
323	38.243	105.984	L	2.6	L	19	0.84	19	L	63	L	8	69.4	18.6	0.30	5600	0.7	2.0	0.5	1.0	L
324	38.243	105.986	L	3.2	L	18	0.78	19	L	61	L	8	74.5	20.2	0.35	5600	1.0	2.0	0.3	0.7	L
325	38.242	105.987	L	1.9	0.280	18	1.20	20	L	79	L	16	72.5	19.5	0.41	5390	0.3	2.0	0.5	1.5	L
326	38.242	105.988	L	2.1	0.280	19	1.00	23	L	84	L	16	70.6	18.9	0.29	5432	0.2	2.0	0.2	1.0	L
327	38.242	105.990	L	2.3	0.290	18	0.88	25	L	77	L	11	75.8	20.5	0.41	5560	0.3	2.0	0.3	1.0	L
328	38.241	105.992	L	2.3	0.220	16	0.97	26	L	69	L	50	73.0	19.7	0.28	5440	0.3	3.0	0.3	1.5	L
329	38.241	105.992	L	2.8	L	20	0.91	19	L	65	20	9	75.2	20.4	0.37	5600	0.2	2.0	0.3	1.5	L
330	38.241	105.993	L	3.0	0.061	19	1.20	22	L	74	L	10	72.0	19.4	0.31	5180	0.2	2.0	0.3	1.5	L
331	38.241	105.996	0.310	2.1	0.320	18	1.10	30	L	85	L	119	71.3	18.6	0.53	5252	0.3	2.0	0.3	1.5	0.2
332	38.240	105.998	0.097	2.4	0.130	21	1.10	26	L	90	L	25	73.8	19.8	0.39	5390	0.2	3.0	0.5	1.0	L

Appendix A. Results of analyses of samples near Villa Grove. "L" = not detected at lowest level of determination.

Number	Lat	Long	xAg	xAs	xCd	xCu	xMo	xPb	xSb	xZn	Hg	H+	N2	O2	CO2	He	Ca	Fe	Mg	Na	P
333	38.240	105.998	L	1.8	L	19	0.95	19	L	77	L	11	72.6	19.7	0.36	5390	0.2	3.0	0.5	1.0	L
334	38.240	105.999	L	2.3	0.190	18	0.97	21	L	83	20	7	69.7	18.7	0.33	5390	0.2	2.0	0.3	1.5	L
335	38.240	106.000	L	2.7	0.150	19	1.00	20	L	80	L	6	72.8	19.6	0.47	5348	0.3	2.0	0.3	1.0	L
336	38.240	106.002	L	3.7	L	19	0.89	18	L	63	30	8	74.1	20.0	0.24	5348	1.5	2.0	0.5	1.5	L
337	38.239	106.005	L	4.1	L	17	0.85	17	L	84	20	7	72.8	19.6	0.37	5348	1.5	1.5	0.3	1.0	L
338	38.239	106.008	L	3.8	L	20	0.83	17	L	72	30	7	73.3	19.8	0.41	5306	1.0	2.0	0.5	1.0	L
339	38.238	106.010	0.120	4.3	L	21	1.00	22	L	93	20	6	B	B	B	B	0.3	3.0	0.5	1.0	L
340	38.238	106.013	L	2.7	0.092	18	0.95	22	L	120	L	6	70.4	18.5	0.57	5516	0.3	2.0	0.3	1.0	L
341	38.237	106.014	L	3.3	0.094	19	0.92	20	L	76	30	6	69.5	18.7	0.33	5348	0.3	1.5	0.2	0.7	L
342	38.236	106.016	L	3.3	L	23	0.85	17	L	64	20	6	72.1	19.4	0.31	5264	0.5	1.5	0.3	1.5	L
343	38.235	106.017	L	2.7	L	21	0.85	18	L	82	20	3	71.7	19.3	0.17	5348	0.7	1.5	0.3	1.0	L

Appendix A. Results of analyses of samples near Villa Grove. "L" = not detected at lowest level of determination.

Number	Ti	Ag	B	Ba	Be	Co	Cr	Cu	Ga	La	Mn	Nb	Ni	Pb	Sc	Sr	V	Y	Zn	Zr
121	0.3	L	10	700	1.5	10	20	30	20	50	500	L	15	50	7	150	50	20	L	200
122	0.3	0.05	10	700	1.0	15	20	30	15	50	700	L	20	50	7	150	70	15	L	150
123	0.3	L	10	700	1.0	15	30	30	20	50	500	L	15	50	7	150	70	20	L	300
124	0.3	1.00	10	1000	1.0	15	70	50	30	50	500	L	15	150	7	150	70	15	L	150
125	0.3	0.70	10	1000	1.0	15	30	50	30	50	700	L	15	150	7	150	70	15	200	150
126	0.3	L	10	1000	1.0	15	50	30	30	L	700	L	15	70	7	150	70	20	L	200
127	0.3	L	10	1000	1.0	20	70	30	30	50	700	L	20	100	7	200	100	20	L	300
128	0.3	L	10	700	L	10	30	30	20	L	700	L	15	100	5	100	70	15	L	300
129	0.3	L	L	1000	1.0	15	50	30	30	50	700	L	15	70	7	150	100	15	L	300
130	0.3	L	10	1000	1.5	15	30	30	30	50	700	L	15	100	7	200	70	20	200	150
131	0.3	L	L	1000	1.0	20	50	30	30	50	500	L	15	100	7	150	70	20	L	150
132	0.3	L	L	1000	1.0	15	30	30	20	50	500	L	15	50	7	150	70	20	L	300
133	0.3	L	L	1000	L	15	100	30	20	50	500	20	20	70	7	150	100	15	L	300
134	0.3	L	10	1000	1.5	10	30	30	30	50	700	L	15	150	5	150	70	15	L	300
135	0.3	L	L	1000	1.0	20	50	30	20	50	500	20	15	100	7	150	70	20	L	300
136	0.5	2.00	10	1500	1.0	20	70	30	30	50	700	20	20	70	7	200	100	20	L	300
137	0.3	L	L	1000	1.0	15	50	20	30	50	700	20	15	100	7	200	70	20	L	200
138	0.3	L	L	1000	1.0	15	30	20	30	50	700	L	20	70	7	150	70	15	L	200
139	0.3	L	L	1000	1.0	15	50	20	20	50	500	20	15	50	7	150	70	20	L	300
140	0.3	L	10	1000	1.5	15	70	30	30	50	700	20	20	50	7	200	70	20	L	300
141	0.3	L	10	700	1.0	15	50	20	20	50	300	20	15	30	7	200	70	20	L	200
142	0.3	L	L	700	1.0	15	50	20	30	50	300	L	15	50	7	150	70	20	L	200
143	0.5	L	10	1000	1.5	15	50	30	30	50	500	L	15	100	7	200	70	20	L	300
305	0.3	L	L	700	1.0	10	30	30	20	50	300	20	20	70	7	200	50	15	L	150
306	0.2	L	L	700	1.0	10	20	15	20	50	300	L	15	30	7	200	50	15	L	100
307	0.3	L	10	700	1.0	10	30	20	20	50	300	L	20	30	7	150	50	15	L	150
308	0.2	L	10	700	1.0	0	50	20	20	50	500	L	15	30	7	200	50	15	L	100
309	0.2	L	10	700	1.0	10	50	15	15	50	500	L	15	30	7	150	50	15	L	100
310	0.2	L	10	700	1.0	10	30	20	15	50	500	L	20	30	7	150	50	15	L	150
311	0.3	L	10	1000	1.5	15	70	30	30	50	700	20	20	50	10	150	70	20	L	200
312	0.2	L	10	700	1.0	10	50	30	30	50	500	L	15	50	7	150	50	20	L	200
313	0.2	L	10	700	1.5	0	20	20	15	50	500	L	15	30	7	150	30	20	L	150
314	0.2	L	L	1000	1.0	15	50	20	30	50	500	L	20	30	7	200	70	20	L	150
315	0.2	L	L	700	1.0	15	50	20	20	50	500	L	20	30	7	200	50	20	L	150
316	0.2	L	L	1000	1.0	10	50	20	30	50	700	L	15	100	7	200	50	20	L	200
317	0.2	L	L	1000	1.0	15	30	20	20	50	500	L	20	30	7	200	50	20	L	150
318	0.2	L	10	1000	1.5	10	70	20	15	50	500	L	15	50	7	200	70	15	L	100
319	0.2	L	10	700	1.0	10	30	20	20	50	500	L	20	30	7	150	50	15	L	200
320	0.2	L	L	700	1.0	10	30	20	20	50	500	L	15	30	7	200	50	15	L	70
321	0.3	L	10	1000	1.0	15	70	20	30	50	500	20	20	30	7	200	70	20	L	300
322	0.3	L	10	700	1.0	10	30	15	10	50	300	L	20	20	7	200	50	20	L	300
323	0.3	L	10	500	1.0	10	20	20	15	50	500	L	20	30	7	200	50	20	L	200
324	0.3	L	10	500	1.0	10	15	15	10	50	500	L	15	20	7	200	70	15	L	150
325	0.5	L	10	700	1.0	15	50	20	20	50	700	20	20	50	7	200	50	20	L	200
326	0.3	L	10	500	1.0	10	30	20	15	50	500	20	15	30	7	150	50	20	L	150
327	0.3	L	10	700	1.0	10	30	20	20	50	500	20	20	30	7	200	50	20	L	300
328	0.3	L	10	1000	1.0	10	70	30	30	50	500	20	15	50	7	200	70	20	L	200
329	0.2	L	10	700	1.5	10	50	20	20	50	500	L	20	30	7	150	30	15	L	100
330	0.3	L	10	700	1.0	10	30	20	30	50	500	20	20	50	7	150	50	20	L	150
331	0.3	L	10	700	1.5	10	50	20	30	50	500	20	20	50	7	200	50	20	L	200
332	0.3	L	10	700	1.0	15	30	20	20	50	500	20	20	30	7	200	50	20	L	150

Appendix A. Results of analyses of samples near Villa Grove. "L" = not detected at lowest level of determination.

Number	Ti	Ag	B	Ba	Be	Co	Cr	Cu	Ga	La	Mn	Nb	Ni	Pb	Sc	Sr	V	Y	Zn	Zr
333	0.5	L	15	700	1.0	15	50	20	20	50	700	30	20	30	7	100	70	30	L	300
334	0.2	L	10	700	1.0	10	50	20	20	50	500	L	20	30	7	150	50	15	L	200
335	0.3	L	10	700	1.5	10	70	20	15	50	500	20	20	20	7	150	50	20	L	150
336	0.2	L	15	700	1.0	10	30	30	20	50	500	L	20	30	7	150	30	20	L	150
337	0.2	L	10	700	1.0	10	10	15	10	50	500	L	20	20	5	200	30	15	L	100
338	0.2	L	10	700	1.0	10	50	20	20	50	500	L	20	30	7	200	50	20	L	150
339	0.3	L	10	700	1.0	15	50	30	20	50	500	20	30	30	7	150	70	20	L	300
340	0.2	L	10	500	1.0	10	20	15	15	50	500	L	15	20	7	150	30	15	L	150
341	0.2	L	10	300	1.0	10	15	15	10	50	300	L	15	20	5	150	30	15	L	100
342	0.2	L	10	500	1.0	10	50	20	20	50	300	L	20	20	7	150	30	15	L	70
343	0.2	L	10	500	1.5	10	30	20	30	50	500	L	20	30	7	150	30	15	L	100

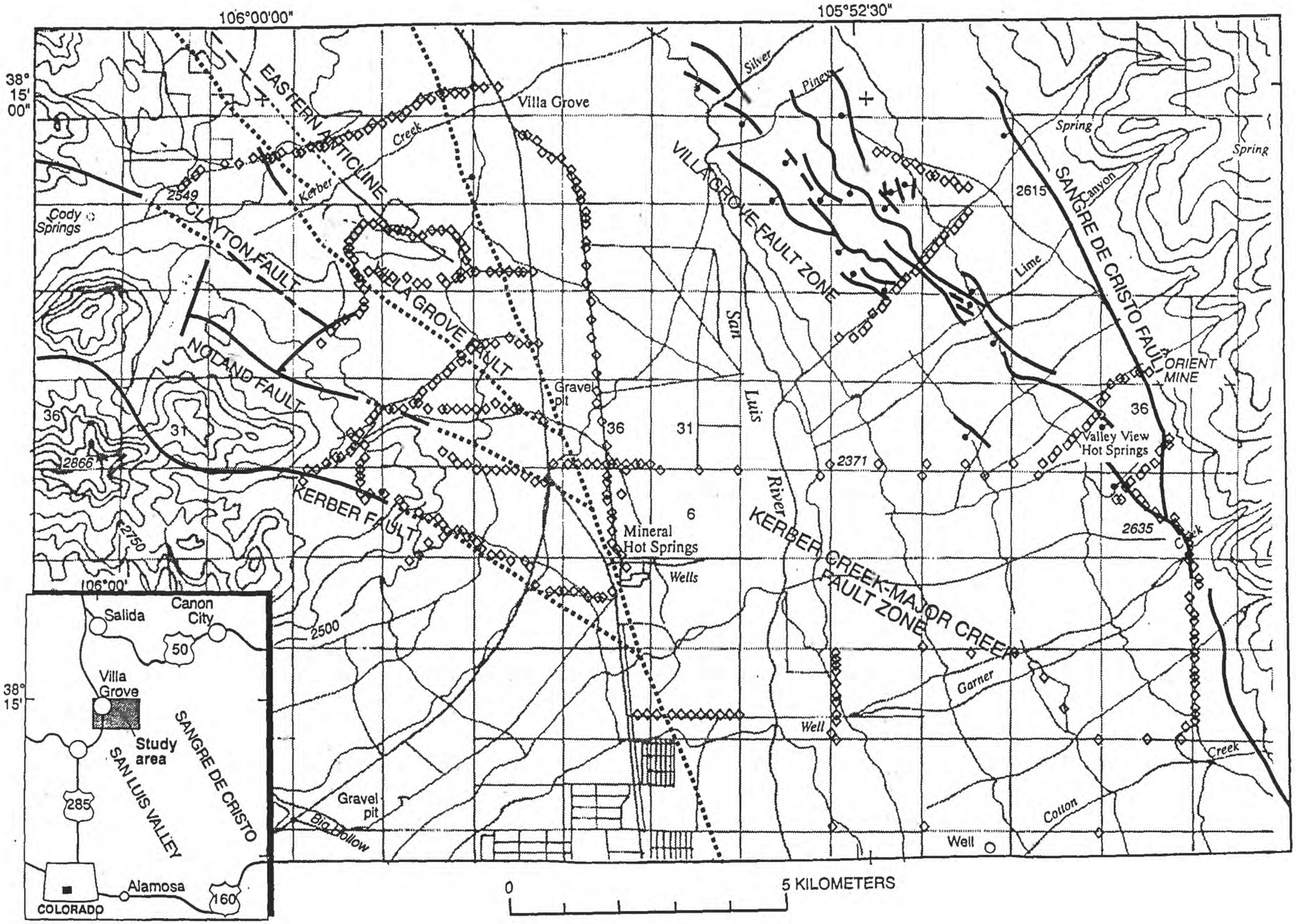

Fig. 1. Location of the study area, showing major faults. Small diamonds are sample sites.

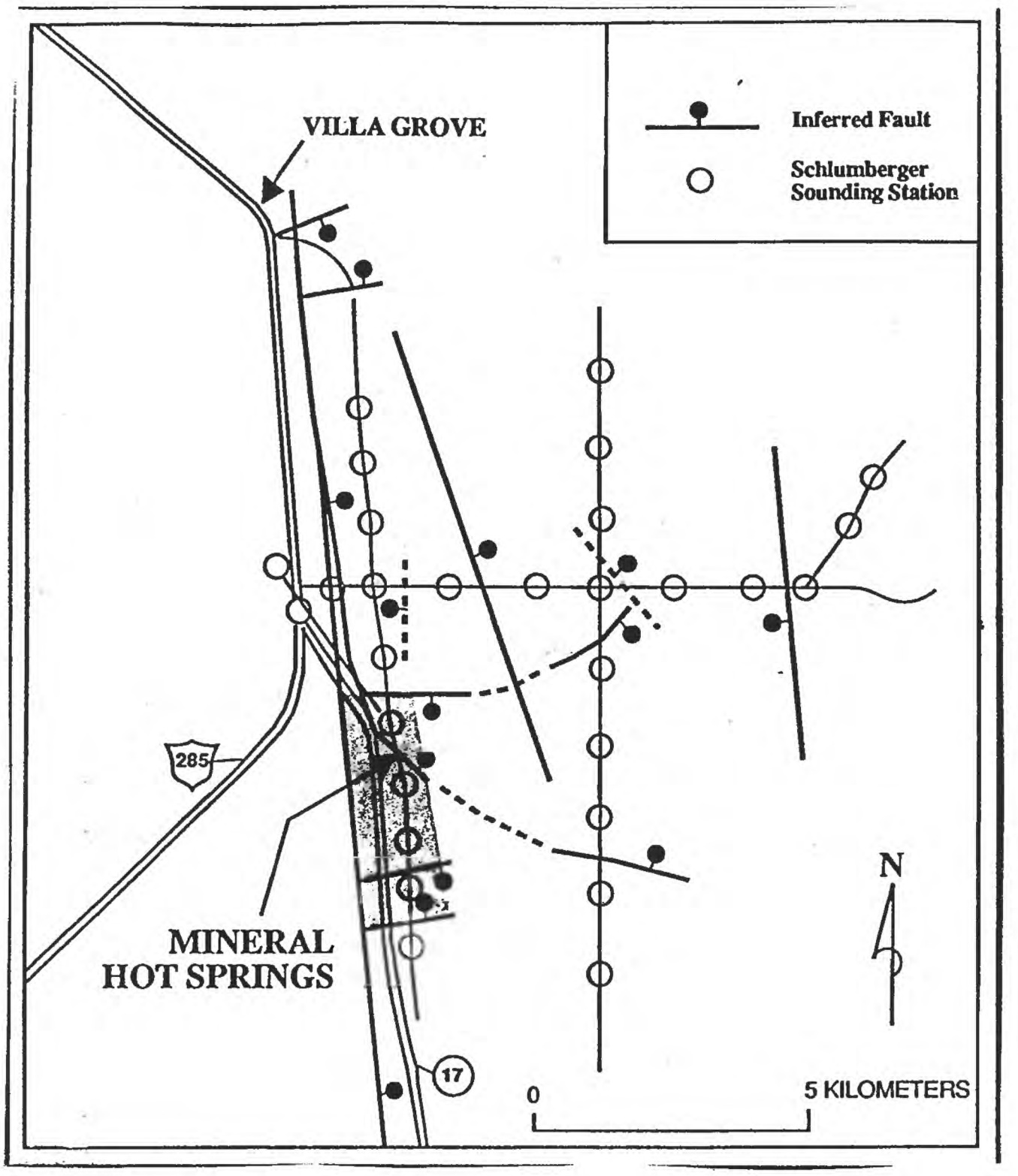

Fig. 2. Locations of inferred faults based on a resistivity study (Zohdy and Bisdorf, 1993). Shaded area is a zone of low resistivity.

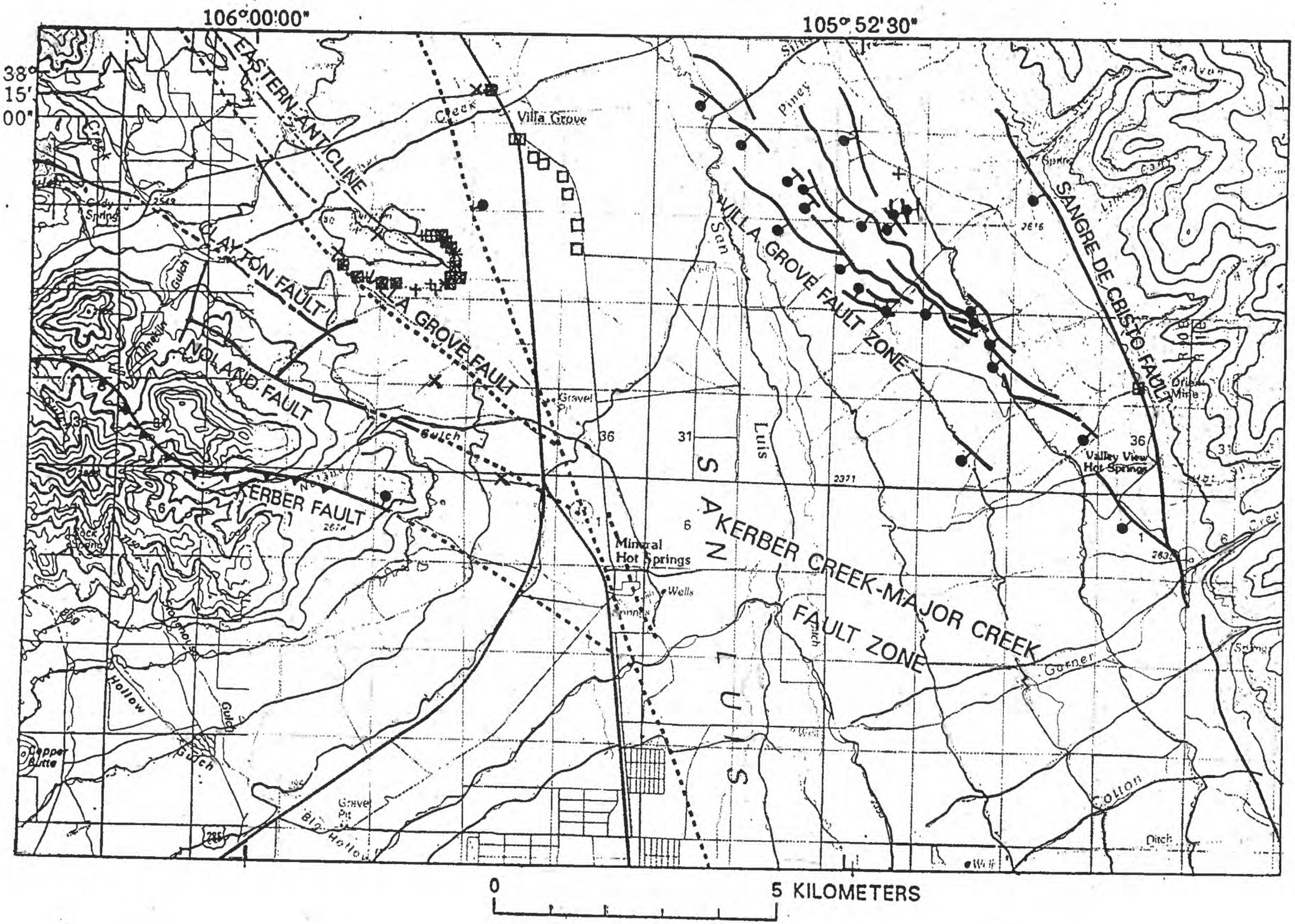

Fig. 3. Concentrations >95th percentiles for (x) As, (+) Sb, and (□) Pb.

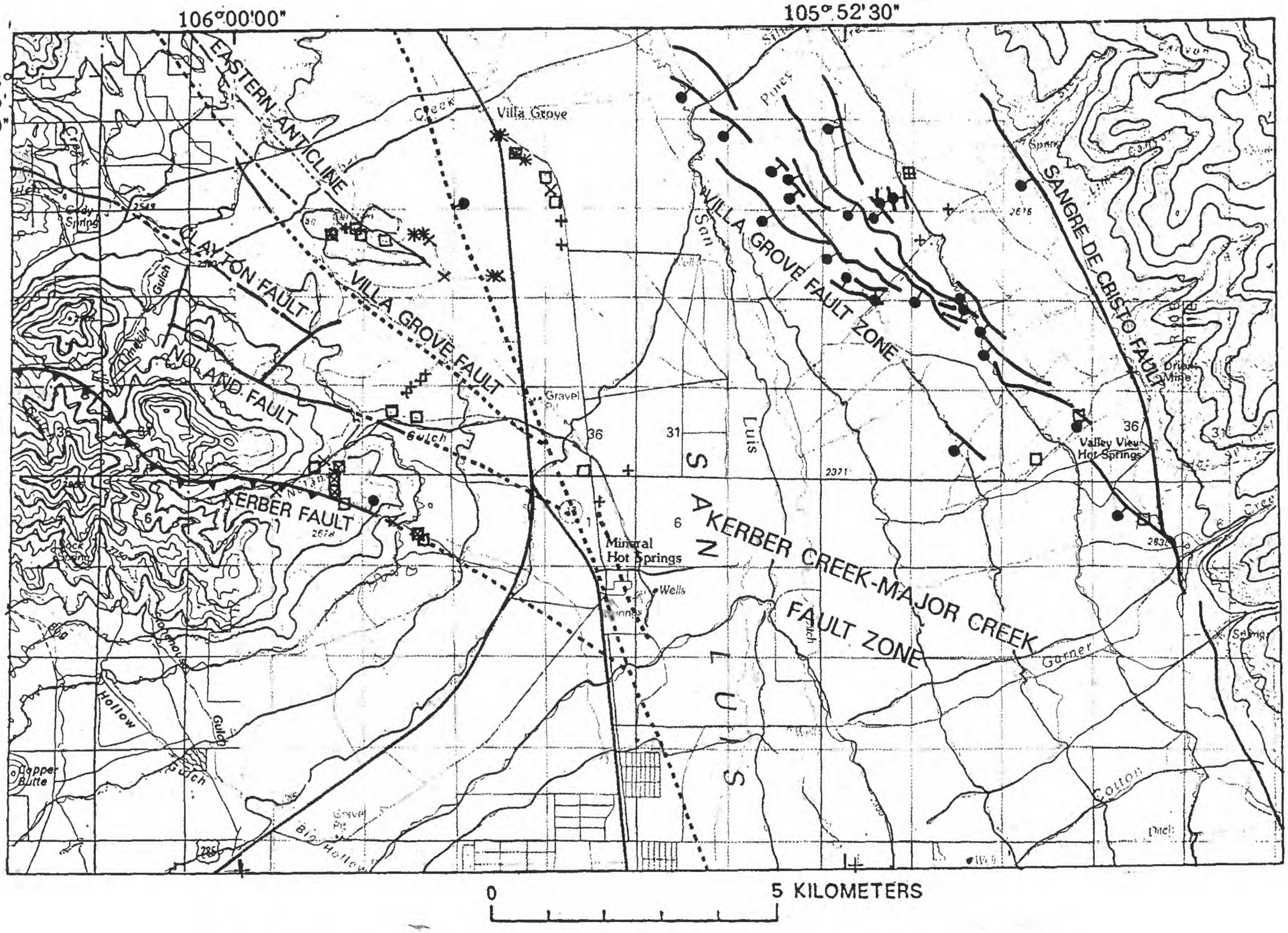

Fig. 4. Concentrations >95th percentiles for (x) Zn, (+) Cd, and (□) H+.

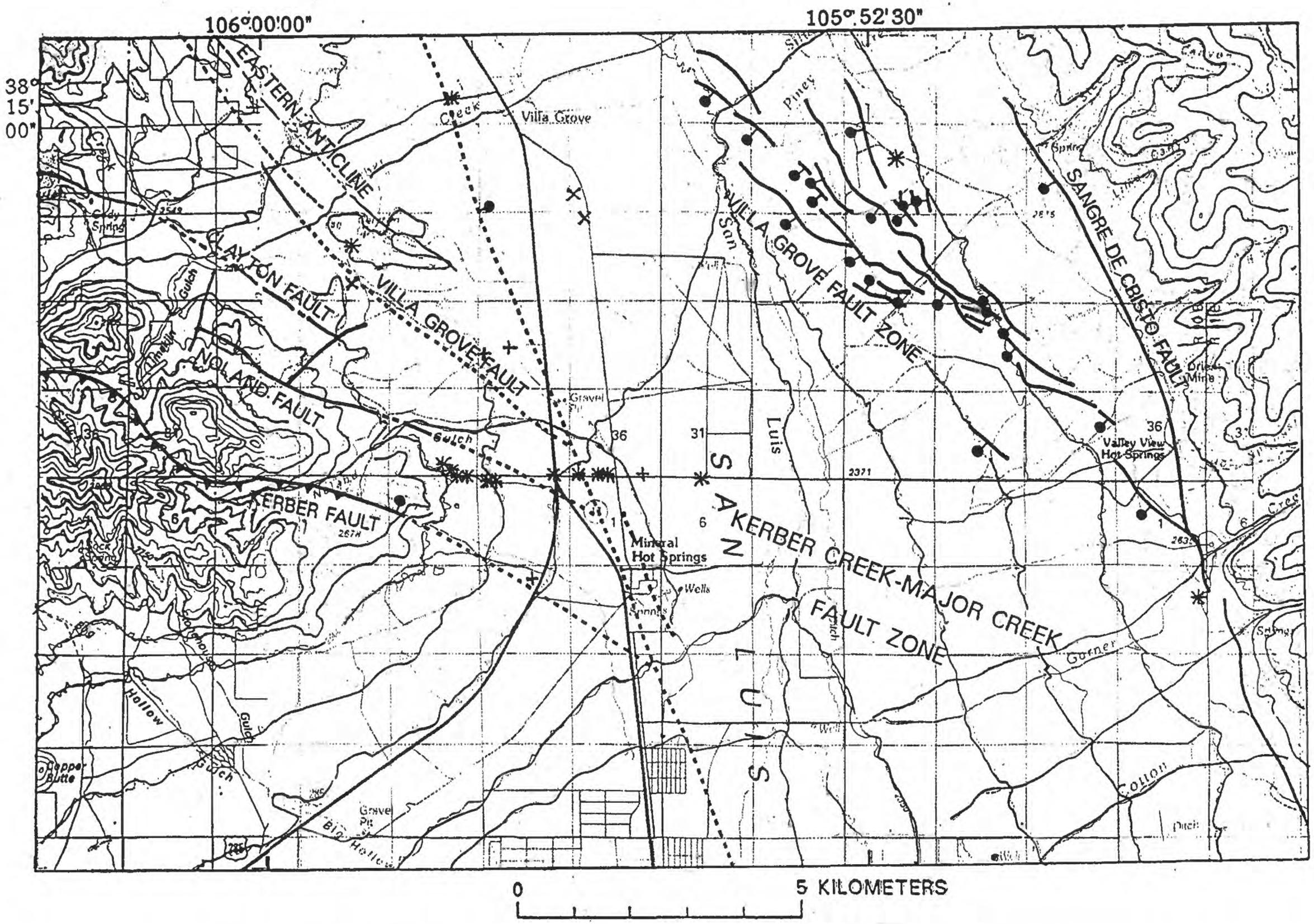

Fig. 5. Concentrations >95th percentiles for (x) N_2 and (+) O_2.

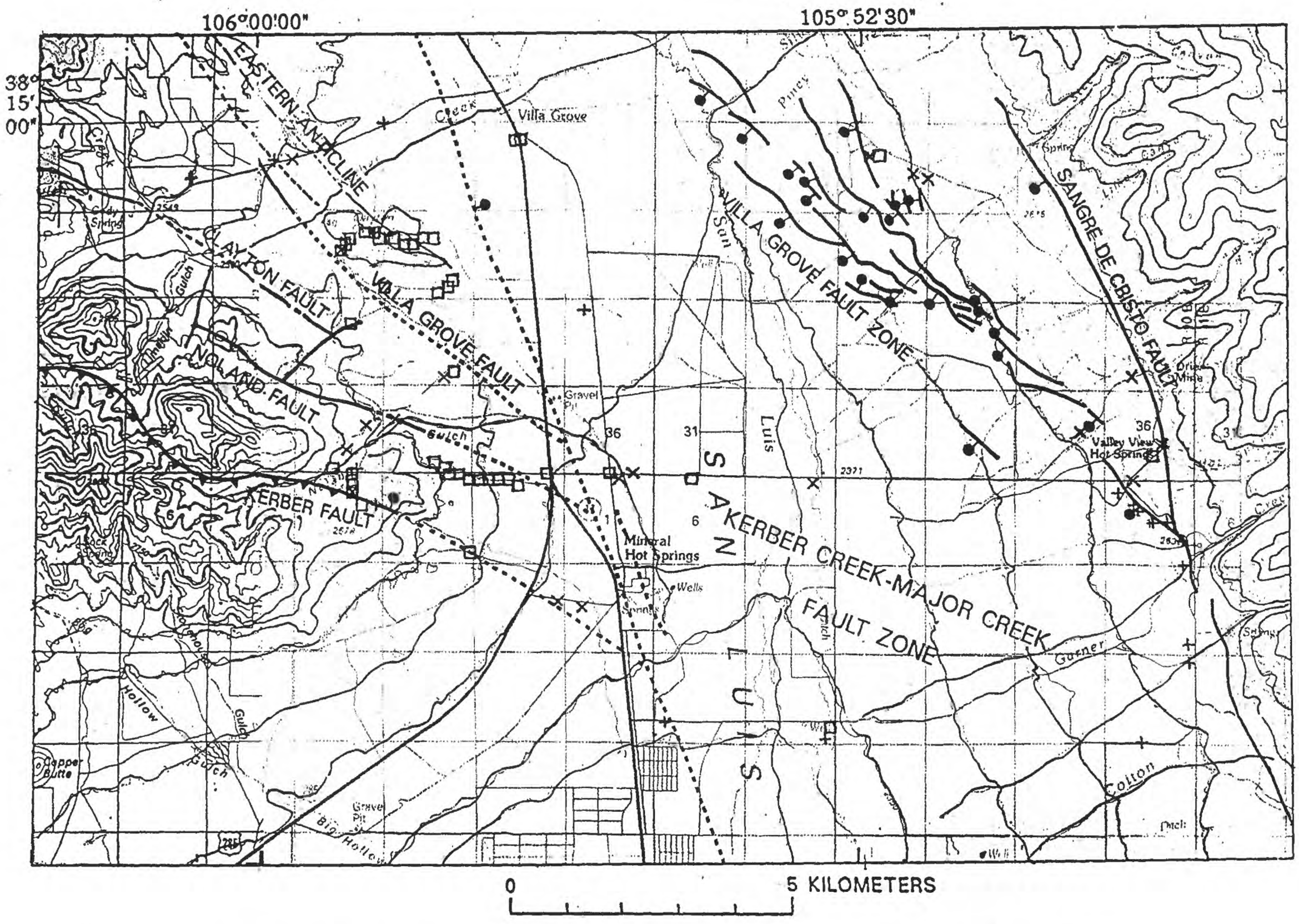

Fig. 6. Concentrations >95th percentiles for (x) He, (+) CO_2, and (□) Hg.

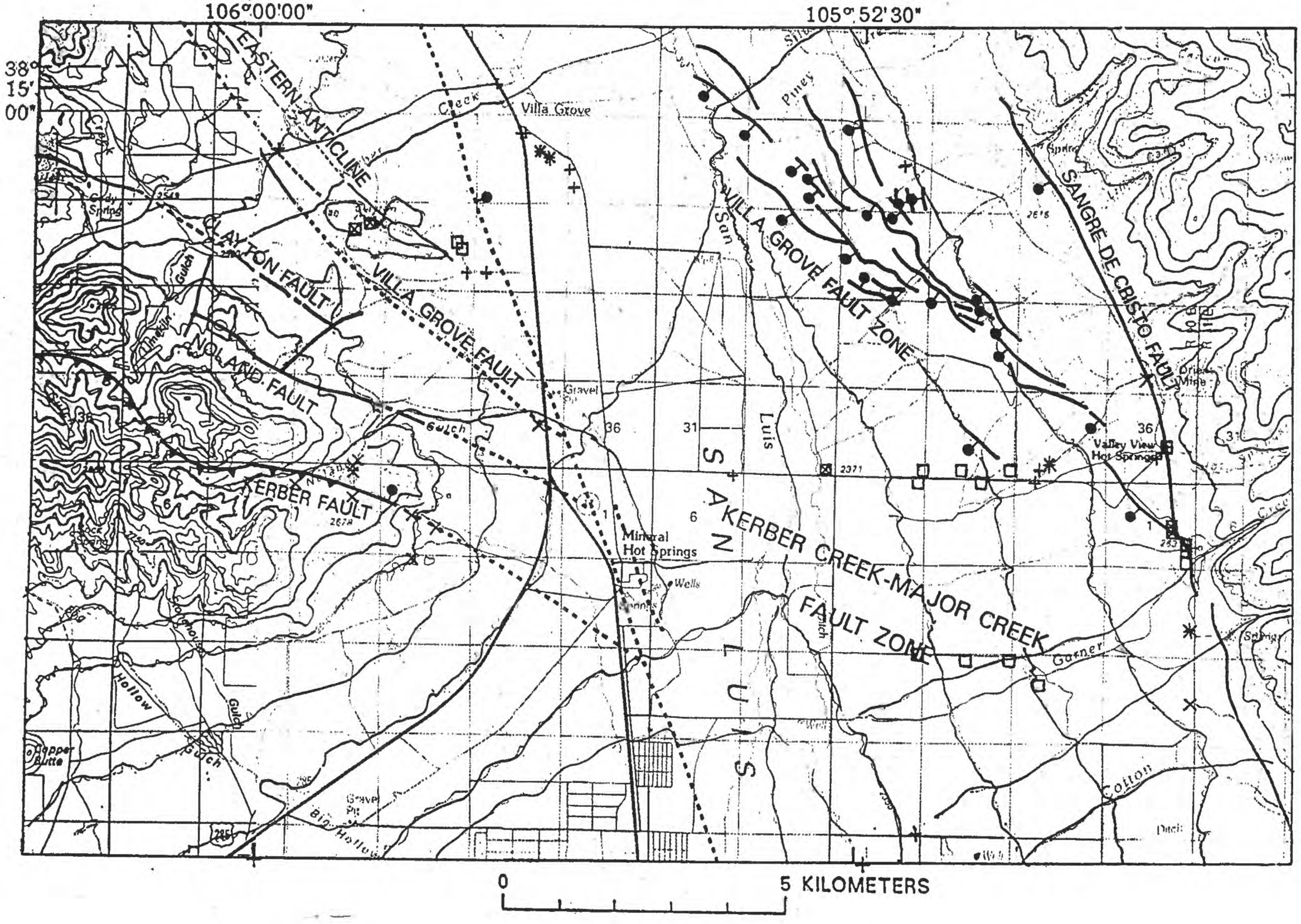

Fig. 7. Concentrations >95th percentiles for (x) Cu, (+) Ag, and (□) Mo.

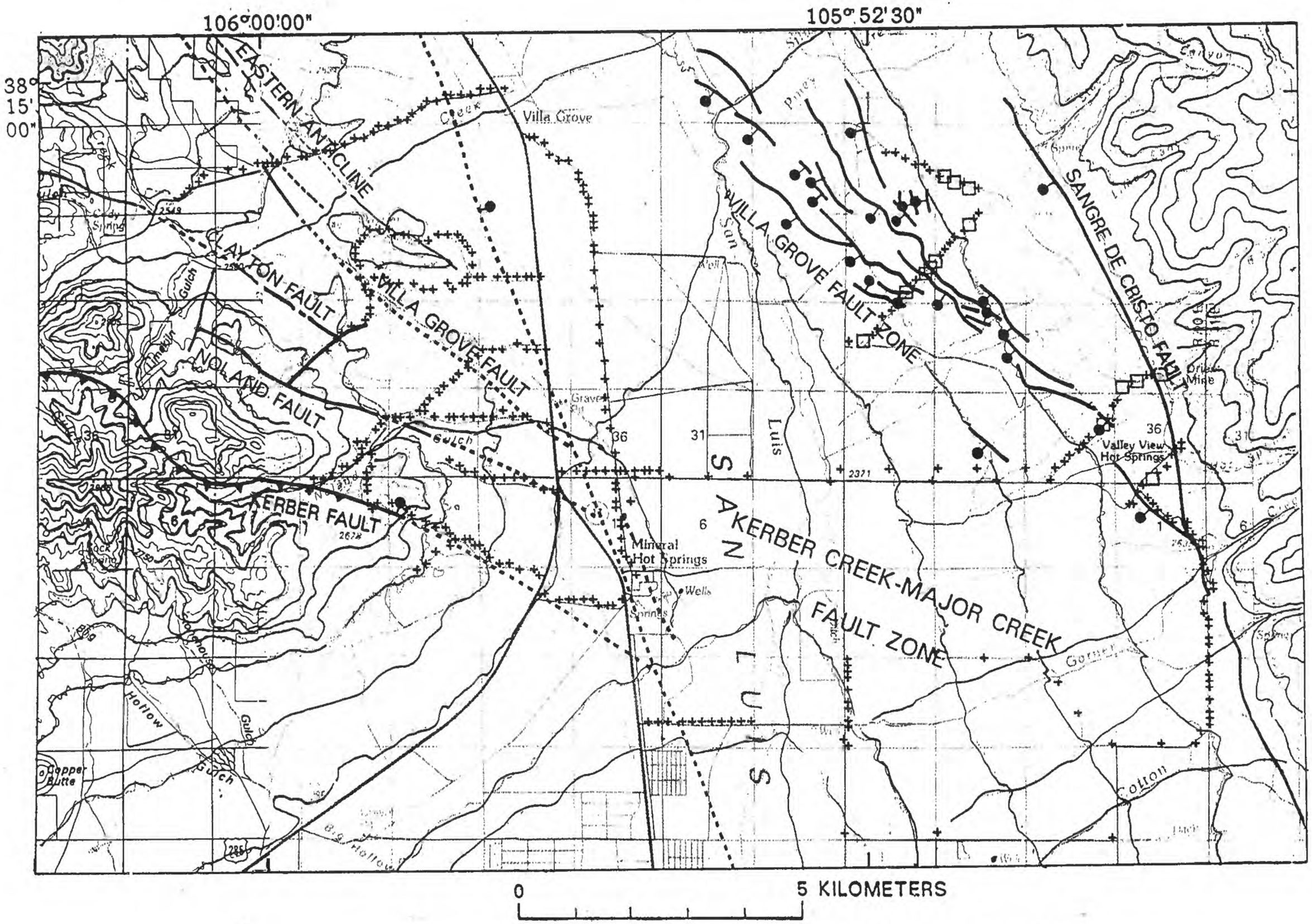

Fig. 8. Ratio of N_2 / O_2. (+) sample sites, (□) N_2 / O_2 > mean + 2 STD.

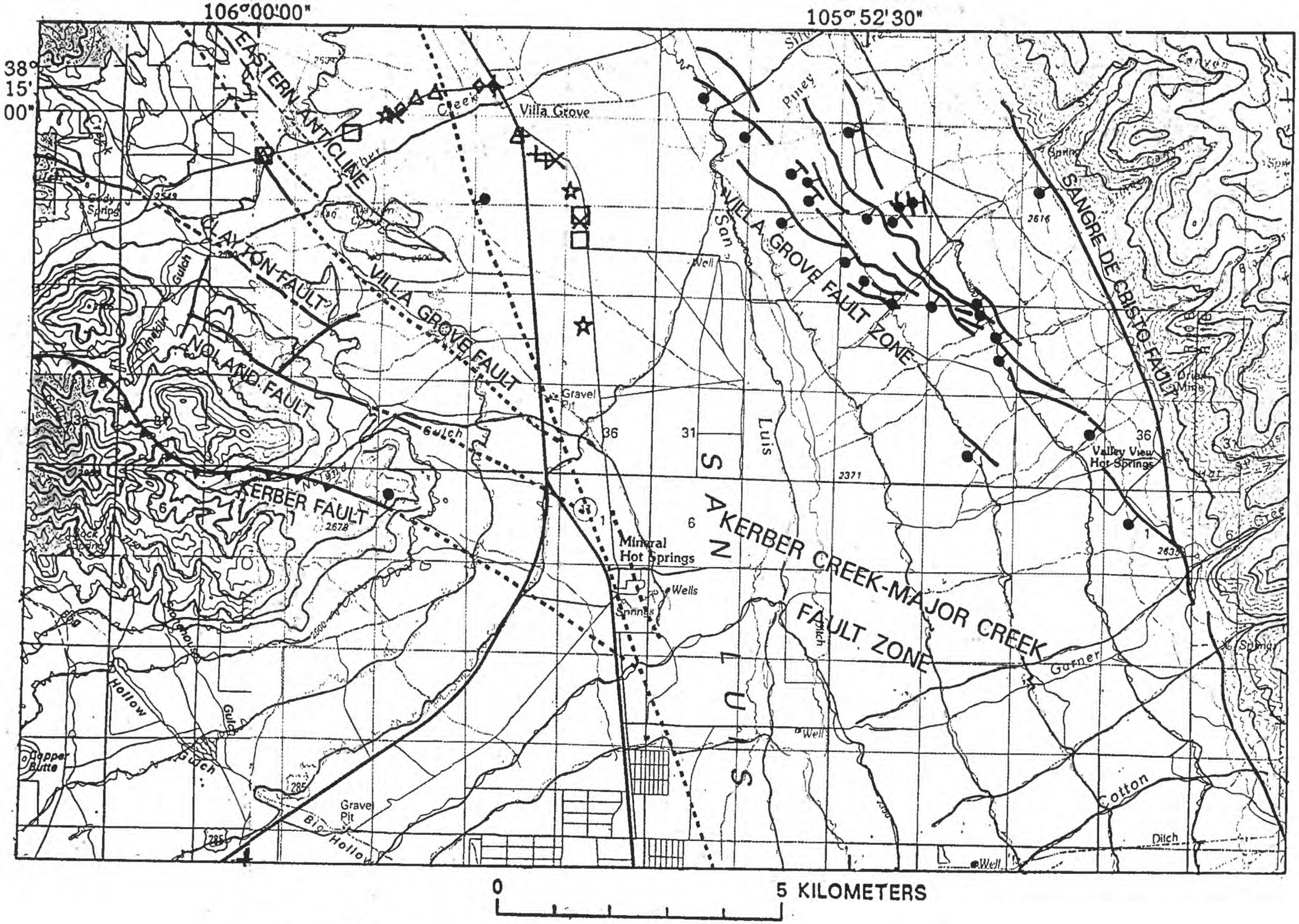

Fig. 9. Villa Grove area: Factor scores (6-factor model) >95th percentiles. (+) factor-1, (□) factor-2, (△) factor-3, (☆) factor-4, (x) factor-5, (◇) factor-6

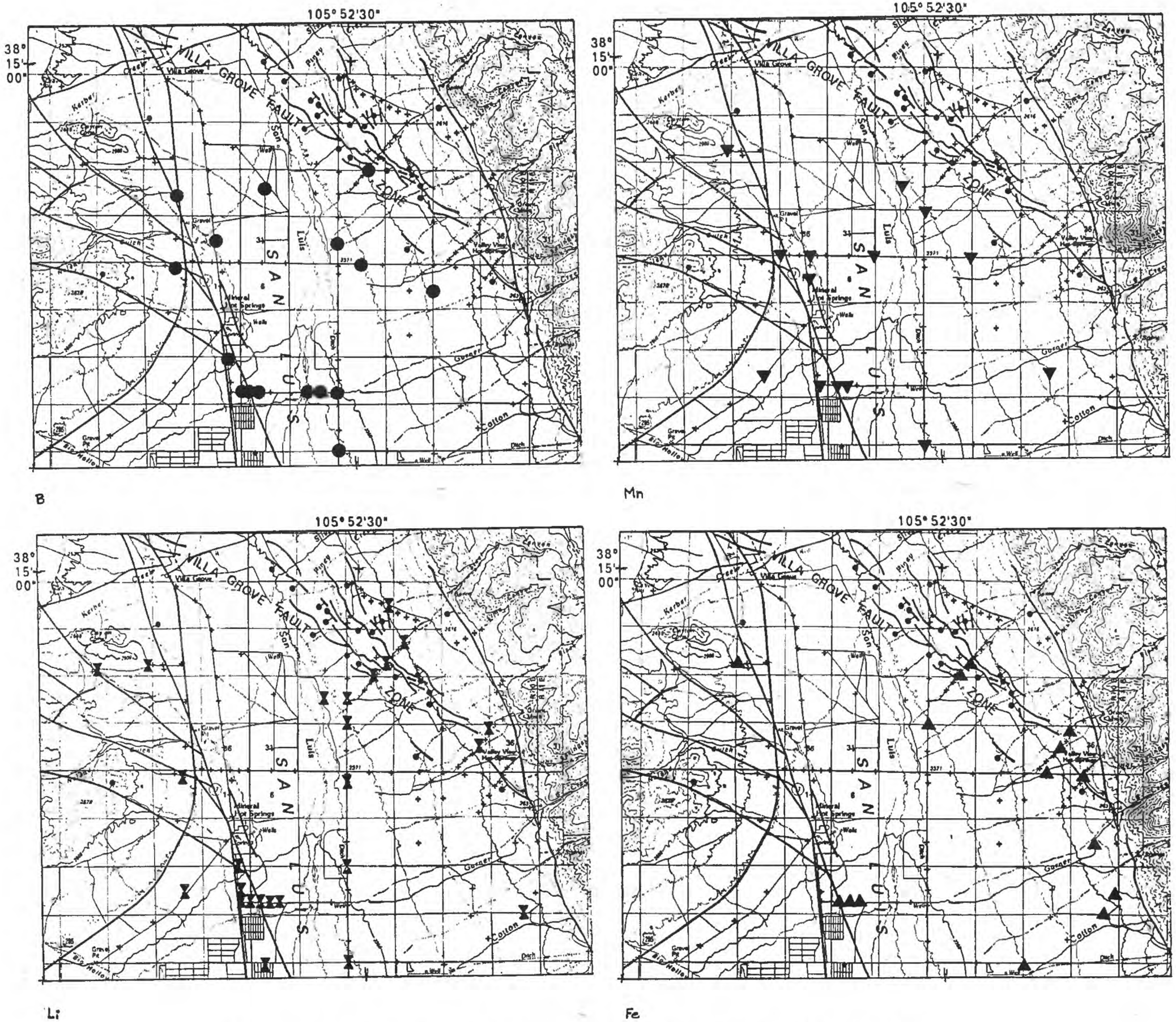

Fig. 10. Concentrations > 90th percentile of elements in rabbitbrush:
▼ Mn (>1200 ppm in ash), ▲ Fe (>0.21% in ash),
⧗ Li (>6.1 ppm in ash), ● B (>6.2 ppm in dry sample),
(+) sample sites.

Figure 11. The sulfur-indicator plant, wild buckwheat (*Eriogonum effusum*), common on a scarp of the Villa Grove fault zone. The small lens cap rests on a silicified boulder whose face is epidote-covered slickensides, evidence of faulting. Photographed April 25, 1993.